

Carbon–Sulfur Bond-Forming Reductive Elimination Involving sp -, sp^2 -, and sp^3 -Hybridized Carbon. Mechanism, Steric Effects, and Electronic Effects on Sulfide Formation

Grace Mann,[†] David Baranano,[†] John F. Hartwig,^{*,†} Arnold L. Rheingold,[‡] and Ilia A. Guzei[‡]

Contribution from the Department of Chemistry, Yale University, P.O. Box 208107, New Haven, Connecticut 06520-8107, and Department of Chemistry, University of Delaware, Newark, Delaware 19716

Received April 27, 1998

Abstract: Palladium thiolato complexes [(L)Pd(R)(SR')], within which L is a chelating ligand such as DPPE, DPPP, DPPBz, DPPF, or TRANSPHOS, R is a methyl, alkenyl, aryl, or alkynyl ligand, and R' is an aryl or alkyl group, were synthesized by substitution or proton-transfer reactions. All of these thiolato complexes were found to undergo carbon–sulfur bond-forming reductive elimination in high yields to form dialkyl sulfides, diaryl sulfides, alkyl aryl sulfides, alkyl alkenyl sulfides, and alkyl alkynyl sulfides. Reductive eliminations forming alkenyl alkyl sulfides and aryl alkyl sulfides were the fastest. Eliminations of alkynyl alkyl sulfides were slower, and elimination of dialkyl sulfide was the slowest. Thus the relative rates for sulfide elimination as a function of the hybridization of the palladium-bound carbon follow the trend $sp^2 > sp \gg sp^3$. Rates of reductive elimination were faster for cis-chelating phosphine ligands with larger bite angles. Kinetic studies, along with results from radical trapping reactions, analysis of solvent effects, and analysis of complexes with chelating phosphines of varying rigidity, were conducted with [Pd(L)(S-*tert*-butyl)(Ar)] and [Pd(L)(S-*tert*-butyl)(Me)]. Carbon–sulfur bond-forming reductive eliminations involving both saturated and unsaturated hydrocarbyl groups proceed by an intramolecular, concerted mechanism. Systematic changes in the electronic properties of the thiolate and aryl groups showed that reductive elimination is the fastest for electron deficient aryl groups and electron rich arenethiolates, suggesting that the reaction follows a mechanism in which the thiolate acts as a nucleophile and the aryl group an electrophile. Studies with thiolate ligands and hydrocarbyl ligands of varying steric demands favor a migration mechanism involving coordination of the hydrocarbyl ligand in the transition state.

Introduction

Carbon–carbon bond-forming reductive eliminations form the new C–C bond in organic products produced by transition metal-catalyzed cross-coupling reactions. Studies on carbon–carbon bond-forming reductive eliminations have evaluated the relative rates for reactions involving ligands with different degrees of unsaturation.^{1–4} Reductive eliminations that involve unsaturated covalent ligands are rapid, and this favorable rate makes cross-couplings that generate unsaturated organic compounds such as carbonyl compounds, arenes, alkenes, and alkynes useful methodology. Previous studies on reductive elimination involving unsaturated ligands suggested that this type of reductive elimination is rapid because the transition state is stabilized by coordination of the eliminating ligand.^{1,5–8}

Reductive eliminations involving alkyl ligands would be less stabilized by coordination and would, therefore, show slower reaction rates.

Reductive eliminations that form the carbon–heteroatom bonds in amines,^{9–15} ethers,^{13,16} and sulfides^{17,18} are unusual and constitute a new class of organometallic reactions that could be incorporated into a number of catalytic processes.^{10,13,17,19–43}

[†] Yale University.

[‡] University of Delaware.

(1) Collman, J. P.; Hegedus, L. S.; Norton, J. R.; Finke, R. G. *Principles and Applications of Organotransition Metal Chemistry*, 2nd ed.; University Science Books: Mill Valley, CA, 1987; pp 322–333.

(2) Stille, J. K. *Pure Appl. Chem.* **1985**, *57*, 1771–1780.

(3) Stille, J. K. *Angew. Chem., Int. Ed. Engl.* **1986**, *25*, 508–524.

(4) Trost, B. M. In *Comprehensive Organic Synthesis*; Pergamon Press: New York, 1991; Vol. 3, pp 435–520.

(5) Chang, J.; Bergman, R. G. *Organometallics* **1987**, *109*, 4298–4304.

(6) Evitt, E. R.; Bergman, R. G. *J. Am. Chem. Soc.* **1980**, *102*, 7003–7011.

(7) Ozawa, F.; Kurihara, K.; Fujimori, M.; Hidaka, T.; Toyoshima, T.; Yamamoto, A. *Organometallics* **1989**, *8*, 180–188.

(8) Suggs, J. W.; Wovkulich, M. J.; Cox, S. D. *Organometallics* **1985**, *4*, 1101–1107.

(9) (a) Driver, M. S.; Hartwig, J. F. *J. Am. Chem. Soc.* **1995**, *117*, 4708–9; (b) Driver, M. S.; Hartwig, J. F. *J. Am. Chem. Soc.* **1997**, *119*, 8232–45.

(10) Driver, M. S.; Hartwig, J. F. *J. Am. Chem. Soc.* **1996**, *118*, 7217–7218.

(11) Widenhoefer, R. A.; Buchwald, S. L. *Organometallics* **1996**, *15*, 3534–3542.

(12) Hartwig, J. F.; Richards, S.; Baranano, D.; Paul, F. *J. Am. Chem. Soc.* **1996**, *118*, 3626–3633.

(13) Mann, G.; Hartwig, J. F. *J. Am. Chem. Soc.* **1996**, *118*, 13109–13110.

(14) Hartwig, J. F. *Angew. Chem., Int. Ed. Engl.* **1998**, *37*, 2090–3.

(15) Villanueva, L. A.; Abboud, K. A.; Boncella, J. M. *Organometallics* **1994**, *13*, 3921–3931.

(16) (a) Widenhoefer, R. A.; Zhong, H. A.; Buchwald, S. L. *J. Am. Chem. Soc.* **1997**, *119*, 6787–6795. (b) Widenhoefer, R. A.; Buchwald, S. L. *J. Am. Chem. Soc.* **1998**, *120*, 6504–6511.

(17) Baranano, D.; Hartwig, J. F. *J. Am. Chem. Soc.* **1995**, *117*, 2937–2938.

(18) Osakada, K.; Maeda, M.; Nakamura, Y.; Yamamoto, T. *J. Chem. Soc., Chem. Commun.* **1986**, 442–443.

Recently, these reactions have been incorporated into catalytic processes that produce arylamines, ethers, and sulfides. These developments in new catalytic methodology have generated questions about how steric properties, electronic properties, and ligand hybridization influence the rates for carbon–heteroatom bond-forming reductive eliminations.

The relative rates for carbon–heteroatom bond-forming reductive eliminations involving a full set of ligands with varying degrees of unsaturation—alkyl, alkenyl, aryl, and alkynyl—have not been examined.^{44–46} The participation of all groups in reductive eliminations and an understanding of the relative rates for their reactions are crucial to the generality and selectivity of the hetero cross-coupling chemistry, as well as the involvement of C–X bond-forming reductive eliminations in new catalytic processes. Further, the relative rates for C–X bond-forming reductive eliminations involving sterically dissimilar aryl groups have not been investigated. However, catalytic amination of sterically hindered aryl groups has been conducted, and they often give higher yields than reactions involving less sterically demanding aryl groups.

Reductive elimination of sulfides is the reverse of sulfide oxidative additions. Thus, the concepts revealed from studies on C–S bond-forming processes are relevant to C–S bond cleavage processes that occur in desulfurization reactions. At least one competition study that involved alkenyl vs aryl C–S

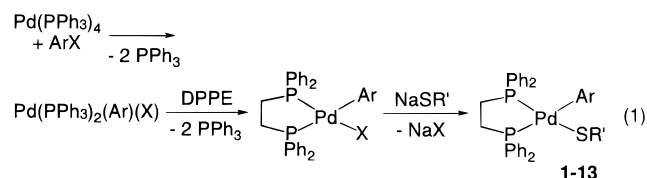
bond cleavage in substituted benzothiophenes⁴⁷ showed a kinetically preferred cleavage of the alkenyl–sulfide portion of the benzothiophene.

The stability and ease of synthesizing palladium thiolato complexes provided a convenient means for studying carbon–heteroatom bond-forming reductive elimination from complexes containing a variety of hydrocarbyl ligands with different electronic and steric properties. In communication form, we reported preliminary results on the reductive elimination of aryl sulfides from palladium thiolato aryl complexes.¹⁷ We report here extensive results on the reductive elimination of sulfides from alkyl, alkenyl, aryl, and alkynyl thiolate complexes, including unusual results with complexes containing sterically distinct aryl groups. These results showed that reductive elimination of sulfide is fastest from alkenyl and aryl complexes, slower for alkynyl complexes, and slowest for alkyl complexes. Further, these studies showed that complexes with bulky alkyl thiolate groups eliminated faster than those with smaller alkyl thiolates, but those with bulky aryl thiolate ligands eliminated slower than those with smaller aryl thiolates. The effect of ligand hybridization on reductive elimination rates, along with kinetic studies that include a systematic evaluation of electronic and steric properties, suggests a mechanism involving coordination of the hydrocarbyl ligand during the transition state for reductive elimination of sulfides.

Results

The Results section first presents synthetic information on the preparation of a variety of palladium thiolate complexes. These complexes contain different hydrocarbyl groups bound to palladium, both alkane and arenethiolates, and different chelating phosphines. Following this synthetic data, information on the reductive elimination chemistry of these complexes is presented. This section on reaction chemistry presents kinetic and mechanistic information along with effects of perturbing structural and electronic properties on the reductive elimination rates. These structural and electronic properties include the bite angle of the phosphine, the steric demands of the palladium-bound aryl group and the thiolate alkyl or aryl group, and the electronic features of the palladium-bound and thiolate aryl groups. The discussion section provides a mechanistic interpretation of these results.

A. Synthesis of Palladium(II) Thiolato Complexes. 1. DPPE–Palladium Thiolato Complexes. The synthesis of [Pd(DPPE)(Ar)(SR')] is summarized in eq 1 (DPPE = 1,2-bis-



R' = *t*-Bu:

- | | |
|--|---|
| 1, Ar = C ₆ H ₅ | 8, Ar = C ₆ H ₄ -3-NH ₂ |
| 2, Ar = C ₆ H ₄ -4-CH ₃ | 9, Ar = C ₆ H ₄ -4-CF ₃ |
| 3, Ar = C ₆ H ₄ -3-CH ₃ | 10, Ar = C ₆ H ₃ -2,4-(CH ₃) ₂ |
| 4, Ar = C ₆ H ₄ -4-Cl | 11, Ar = C ₆ H ₃ -3,4-(CH ₃) ₂ |
| 5, Ar = C ₆ H ₄ -4-OMe | 12, Ar = C ₆ H ₃ -2,6-(CH ₃) ₂ |
| 6, Ar = C ₆ H ₄ -3-OMe | R' = Me: |
| 7, Ar = C ₆ H ₄ -4-NH ₂ | 13, Ar = C ₆ H ₄ -4-Cl |

(diphenylphosphino)ethane). Oxidative addition of aryl halide to [Pd(PPh₃)₄] followed by displacement of the PPh₃ with DPPE resulted in formation of DPPE-ligated palladium aryl halide

- (19) Hartwig, J. F. *Synlett* **1997**, 329–340.
 (20) Louie, J.; Driver, M. S.; Hamann, B. C.; Hartwig, J. F. *J. Org. Chem.* **1997**, *62*, 1268–1273.
 (21) Louie, J.; Hartwig, J. F. *J. Am. Chem. Soc.* **1997**, *119*, 11695–11696.
 (22) Wolfe, J.; Buchwald, S. L. *J. Org. Chem.* **1997**, *62*, 1264–1267.
 (23) Wolfe, J. P.; Ahman, J.; Sadighi, J. P.; Buchwald, S. L. *Tetrahedron Lett.* **1997**, *38*, 6367–6370.
 (24) Wolfe, J. P.; Buchwald, S. L. *J. Am. Chem. Soc.* **1997**, *119*, 6054–6058.
 (25) Wolfe, J. P. *J. Org. Chem.* **1997**, *62*, 6066–6068.
 (26) Ahman, J.; Buchwald, S. L. *Tetrahedron Lett.* **1997**, *38*, 6363–6366.
 (27) The first Pd-catalyzed amination of aryl chlorides was recently published. Beller, M.; Riermeier, T. H.; Reisinger, C.-P.; Herrmann, W. A. *Tetrahedron Lett.* **1997**, *38*, 2073–2079.
 (28) Wolfe, J. P.; Wagaw, S.; Buchwald, S. L. *J. Am. Chem. Soc.* **1996**, *118*, 7215–7216.
 (29) Wolfe, J. P.; Rennels, R. A.; Buchwald, S. L. *Tetrahedron* **1996**, *52*, 7525–7546.
 (30) (a) Wagaw, S.; Buchwald, S. L. *J. Org. Chem.* **1996**, *61*, 7240–7241. (b) Wagaw, S.; Yang, B. H.; Buchwald, S. L. *J. Am. Chem. Soc.* **1998**, *120*, 6621–6622.
 (31) Marcaux, B. S. L. *Abstracts of Papers*, 213th National Meeting of the American Chemical Society, 1997; American Chemical Society: Washington DC, 1997; ORGN 005.
 (32) Zhao, S. H.; Miller, A. K.; Berger, J.; Flippin, L. A. *Tetrahedron Lett.* **1996**, *37*, 4463–4466.
 (33) Cristau, H.; Desmurs, J. *Ind. Chem. Libr.* **1995**, *7*, 249–263.
 (34) Guram, A. S.; Rennels, R. A.; Buchwald, S. L. *Angew. Chem., Int. Ed. Engl.* **1995**, *34*, 1348–1350.
 (35) Louie, J.; Hartwig, J. F. *Tetrahedron Lett.* **1995**, *36*, 3609–3612.
 (36) Cramer, R.; Coulson, R. *J. Org. Chem.* **1975**, *40*, 2267–2273.
 (37) Mann, G.; Hartwig, J. F. *J. Org. Chem.* **1997**, *62*, 5413–5418.
 (38) Mann, G.; Hartwig, J. F. *Tetrahedron Lett.* **1997**, *119*, 8005–8008.
 (39) Palucki, M.; Wolfe, J. P.; Buchwald, S. *J. Am. Chem. Soc.* **1997**, *119*, 3395–3396.
 (40) Palucki, M.; Wolfe, J. P.; Buchwald, S. L. *J. Am. Chem. Soc.* **1996**, *118*, 10333–10334.
 (41) Barton, D. H. R.; Finet, J.; Khamsi, J.; Pichon, C. *Tetrahedron Lett.* **1986**, 3619–3622.
 (42) Parshall, G. W. *Homogeneous Catalysis*; Wiley-Interscience: New York, 1980.
 (43) Takagi, K. *Chem. Lett.* **1987**, 2221–2224.
 (44) Liou, S. Y.; Gozin, M.; Milstein, D. *J. Chem. Soc., Chem. Commun.* **1995**, 1965–1966.
 (45) Komiya, S.; Ozaki, S.; Shibue, A. *J. Chem. Soc., Chem. Commun.* **1986**, 1555–1556.
 (46) Negishi, E.; Takahashi, T.; Akiyoshi, K. *J. Organomet. Chem.* **1987**, *334*, 181–194.
 (47) Myers, A. W.; Jones, W. D.; McClements, S. M. *J. Am. Chem. Soc.* **1995**, *117*, 11704–11709.

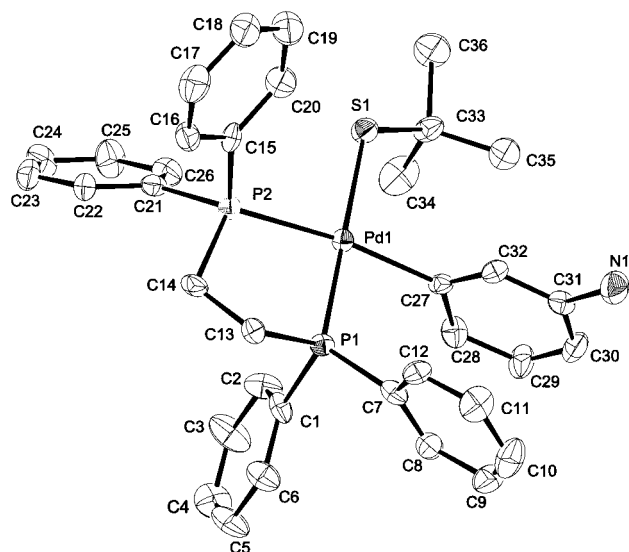


Figure 1. ORTEP drawing of (DPPE)Pd(3-NH₂-C₆H₄)(S-*t*-Bu)·C₇H₈ (**8**). Hydrogen atoms and the solvent molecule are omitted for clarity. Thermal ellipsoids are drawn at 30% probability.

Table 1. Data Collection and Refinement Parameters for X-ray Structure of (DPPE)Pd(3-NH₂-C₆H₄)(S-*t*-Bu)·C₇H₈ (**8**) and (DPPE)Pd(C₆H₅)(S-3,4-(CH₃)₂C₆H₃)·C₄H₈O (**24**)

empirical formula	C ₄₄ H ₃₀ NSP ₂ Pd·C ₇ H ₈ (8)	C ₄₀ H ₃₈ P ₂ PdS·C ₄ H ₈ O (24)
formula weight	770.20	791.21
crystal color, habit	yellow, plate	yellow, block
crystal system	monoclinic	monoclinic
lattice parameters	<i>a</i> = 15.337(6) Å <i>b</i> = 11.619(6) Å <i>c</i> = 22.14(1) Å <i>β</i> = 101.50(4)°	<i>a</i> = 16.7531(5) Å <i>b</i> = 12.0390(4) Å <i>c</i> = 18.9752(7) Å <i>β</i> = 94.991(2)°
volume	3866(3) Å ³	3812.6(2) Å ³
space group	<i>P</i> 2 ₁ / <i>n</i>	<i>P</i> 2 ₁ / <i>n</i>
Z value	4	4
diffractometer	Rigaku AFC5S	Siemens P4/CCD
radiation	MoKα (λ = 0.71069 Å)	MoKα (λ = 0.71073 Å)
<i>T</i>	213(1) K	198(2) K
residuals	<i>R</i> (<i>F</i>), <i>R</i> (<i>wF</i> ²): 4.8%; 5.5%	<i>R</i> (<i>F</i>), <i>R</i> (<i>wF</i> ²): 6.02%; 14.20%
goodness-of-fit on <i>F</i> ²	1.27	1.116

complexes, which were isolated after precipitation with pentane. Monomeric thiolate complexes **1–8** and **10–13** were then generated by addition of sodium alkyl thiolate to THF solutions of DPPE-ligated palladium aryl halide complexes, and the organopalladium thiolates were isolated as yellow crystalline solids in 34–70% yields. These complexes were characterized by ¹H NMR, ³¹P{¹H} NMR, and IR spectroscopy, as well as elemental analysis. Complex **9** was too reactive to isolate. It was, therefore, generated in solution and characterized by solution spectroscopic methods. With the exception of **9**, these compounds were only mildly air sensitive, and were water stable. In the absence of added phosphine ligand, these complexes turned green in solution after several hours at room temperature.

Recrystallization of **8** by slow diffusion of pentane into a toluene solution at –35 °C gave thin crystals of the toluene solvate that were suitable for analysis by X-ray diffraction; an ORTEP diagram is included in Figure 1. Data collection and refinement parameters and selected bond distances and angles are included in Tables 1–3. The geometry around the Pd is planar; the sum of the four angles is 360.0°. The P–Pd–P bite angle is 84.9°, which is similar to the 85.8° angle in [Pd-

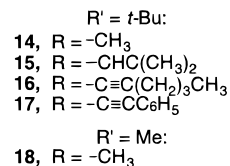
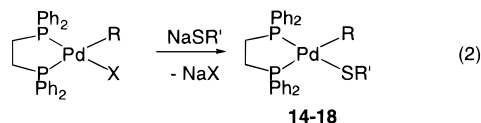
Table 2. Selected Intramolecular Bond Distances Involving the Non-Hydrogen Atoms of (DPPE)Pd(3-NH₂-C₆H₄)(S-*t*-Bu)·C₇H₈ (**8**)

atom–atom	distance, Å	atom–atom	distance, Å
Pd(1)–C(27)	2.053(7)	C(13)–C(14)	1.52(1)
Pd(1)–P(1)	2.256(2)	C(27)–C(28)	1.39(1)
Pd(1)–P(2)	2.360(2)	C(28)–C(29)	1.39(1)
Pd(1)–S(1)	2.371(2)	C(29)–C(30)	1.39(1)
S(1)–C(33)	1.862(8)	C(30)–C(31)	1.38(1)
P(1)–C(7)	1.821(9)	C(31)–N(1)	1.41(1)
P(1)–C(1)	1.836(8)	C(31)–C(32)	1.39(1)
P(1)–C(13)	1.826(8)	C(32)–C(27)	1.38(1)
P(2)–C(15)	1.819(8)	C(33)–C(34)	1.51(1)
P(2)–C(21)	1.832(8)	C(33)–C(35)	1.53(1)
P(2)–C(14)	1.820(7)	C(33)–C(36)	1.53(1)

Table 3. Selected Intramolecular Bond Angles Involving the Non-Hydrogen Atoms of (DPPE)Pd(3-NH₂-C₆H₄)(S-*t*-Bu)·C₇H₈ (**8**)

atom–atom–atom	angle, deg	atom–atom–atom	angle, deg
C(27)–Pd(1)–P(1)	83.9(2)	C(15)–P(2)–Pd(1)	114.4(3)
C(27)–Pd(1)–P(2)	167.9(2)	C(21)–P(2)–Pd(1)	122.3(3)
P(1)–Pd(1)–P(2)	84.89(8)	C(14)–P(2)–Pd(1)	106.1(3)
C(27)–Pd(1)–S(1)	95.7(2)	C(28)–C(27)–Pd(1)	124.8(6)
P(1)–Pd(1)–S(1)	179.45(8)	C(32)–C(27)–Pd(1)	117.2(5)
P(2)–Pd(1)–S(1)	95.49(8)	C(12)–C(7)–P(1)	120.4(6)
C(33)–S(1)–Pd(1)	118.7(3)	C(8)–C(7)–P(1)	120.0(7)
C(1)–P(1)–C(7)	106.3(4)	C(14)–C(13)–P(1)	108.1(5)
C(7)–P(1)–Pd(1)	120.8(3)	C(13)–C(14)–P(2)	112.6(5)
C(1)–P(1)–Pd(1)	110.3(3)	S(1)–C(33)–C(34)	108.6(6)
C(13)–P(1)–Pd(1)	108.2(3)	S(1)–C(33)–C(35)	115.6(6)
C(15)–P(2)–C(21)	105.7(3)	S(1)–C(33)–C(36)	104.2(6)

(DPPE)Cl₂].⁴⁸ The Cl–Pd–Cl bond angle in [Pd(DPPE)Cl₂]⁴⁸ is 94.2° while the C(27)–Pd(1)–S(1) bond angle in **8** is slightly larger at 95.7°, presumably due to the large *tert*-butyl group on the thiolate. The angle between the plane defined by Pd(1), S(1), P(1), and P(2) and the plane of the Pd-bound aryl group is 89.1°. The torsion angle defined by C(27), Pd(1), S(1), and C(33) is 28.2°. The Pd(1)–C(27) and Pd(1)–S(1) bond distances are 2.05 and 2.37 Å, respectively.



Equation 2 summarizes the synthesis of palladium methyl, alkenyl, and alkynyl complexes **14–18**, which contain alkanethiolate ligands. Complexes **15–18** were synthesized according to a procedure similar to that for the synthesis of palladium aryl alkyl thiolate complexes except that the first step involved oxidative addition of alkenyl or alkynyl halides to [Pd-(PPh₃)₄]. Complex **14** was synthesized by a route initiated by reaction of [Pd(COD)Cl₂] with tetramethyltin to form [Pd-(COD)(Me)(Cl)].⁴⁹ Subsequent displacement of the COD by DPPE formed [Pd(DPPE)(Me)(Cl)], and reaction of [Pd(DPPE)(Me)(Cl)] with sodium *tert*-butyl thiolate resulted in the formation of complex **14**. Complexes **14** and **16–18** were

(48) Hayashi, T.; Konishi, M.; Kobori, Y.; Kumada, M.; Higuchi, T.; Hirotsu, K. *J. Am. Chem. Soc.* **1984**, *106*, 158–163.

(49) Ladipo, F. T.; Anderson, G. K. *Organometallics* **1994**, *13*, 303–306.

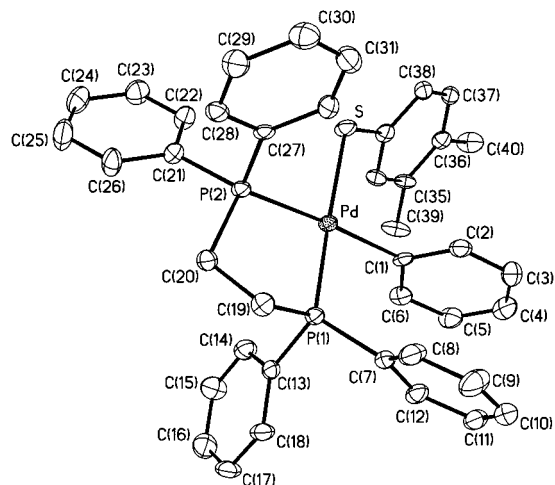
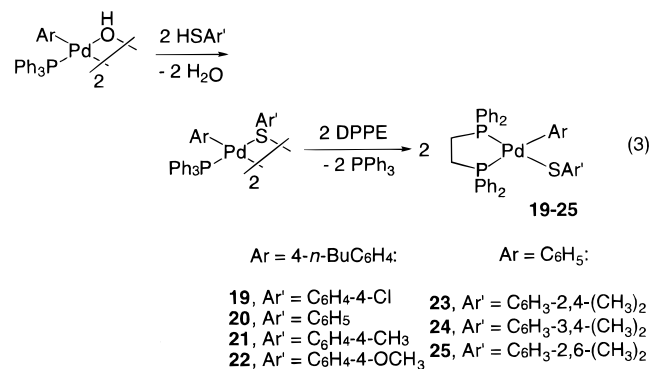


Figure 2. ORTEP drawing of (DPPE)Pd(C₆H₅)(S-3,4-(CH₃)₂C₆H₃)·C₄H₈O (**24**). Hydrogen atoms and solvent molecule are omitted for clarity. Thermal ellipsoids are drawn at 30% probability.

isolated as yellow crystalline solids in 48–86% yields and were characterized by ¹H NMR, ³¹P{¹H} NMR, and IR spectroscopy, as well as elemental analysis. The alkenyl complex **15** was too reactive to isolate in pure form, but was generated in solution and clearly identified by ³¹P{¹H} and ¹H NMR spectroscopy. With the exception of **15**, these complexes are stable for hours at room temperature and are only mildly air sensitive.

2. DPPE–Palladium Aryl Arenethiolato Complexes. Attempts to synthesize palladium aryl arenethiolato complexes by reaction of the sodium arenethiolates with palladium aryl halide complexes gave only low yields of the aryl arenethiolato complexes. However, these complexes were prepared in higher yields by reaction of dimeric PPh₃-ligated palladium hydroxo complexes (eq 3). The *n*-butyl-substituted aryl hydroxo dimer



was synthesized by reaction of [Pd(PPh₃)₂(C₆H₄-4-*n*-Bu)(I)] with cesium hydroxide in THF solvent.⁵⁰ Addition of 2 equiv of the corresponding thiol to a THF solution of the hydroxy dimer resulted in the formation of the thiolato dimer. The thiolato dimer was not isolated, but was treated with 2 equiv of DPPE, which resulted in an orange solution containing the monomeric DPPE-ligated palladium–thiolato complexes **19–22**. These complexes were isolated in 50–86% yield as fluffy pink solids. Arenethiolato complexes **23–25** were generated in 35–52% yields by reaction of [Pd(PPh₃)(Ph)(OH)]₂⁵¹ with the corresponding thiophenol followed by addition of DPPE.

Recrystallization of **24** by slow diffusion of ether into a THF solution at –35 °C gave yellow crystals of the THF solvate

(50) Driver, M. S.; Hartwig, J. F. *Organometallics* **1997**, *16*, 5706–5715.

(51) Grushin, V. V.; Alper, H. *Organometallics* **1993**, *12*, 1890–1901.

Table 4. Selected Intramolecular Bond Distances Involving the Non-Hydrogen Atoms of (DPPE)Pd(C₆H₅)(S-3,4-(CH₃)₂C₆H₃)·C₄H₈O (**24**)

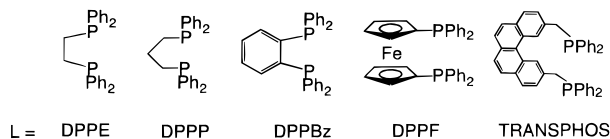
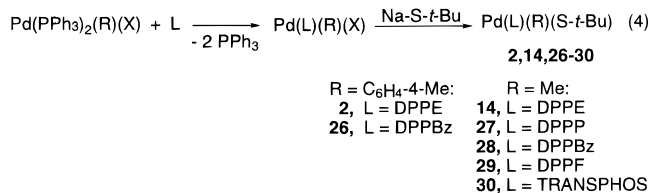
atom–atom	distance, Å	atom–atom	distance, Å
Pd(1)–C(1)	2.041(5)	C(2)–C(3)	1.393(9)
Pd(1)–P(1)	2.256(2)	C(3)–C(4)	1.372(1)
Pd(1)–P(2)	2.3479(1)	C(4)–C(5)	1.365(1)
Pd(1)–S(1)	2.359(2)	C(5)–C(6)	1.397(8)
S(1)–C(33)	1.756(6)	C(6)–C(1)	1.393(8)
P(1)–C(7)	1.810(6)	C(33)–C(34)	1.396(8)
P(1)–C(13)	1.819(6)	C(34)–C(35)	1.398(8)
P(1)–C(19)	1.852(6)	C(35)–C(39)	1.510(9)
P(2)–C(21)	1.825(6)	C(35)–C(36)	1.404(8)
P(2)–C(27)	1.825(6)	C(36)–C(40)	1.507(7)
P(2)–C(20)	1.845(6)	C(36)–C(37)	1.384(8)
C(19)–C(20)	1.511(8)	C(37)–C(38)	1.398(8)
C(1)–C(2)	1.399(8)	C(38)–C(33)	1.384(8)

Table 5. Selected Intramolecular Bond Angles Involving the Non-Hydrogen Atoms of (DPPE)Pd(C₆H₅)(S-3,4-(CH₃)₂C₆H₃)·C₄H₈O (**24**)

atom–atom–atom	angle, deg	atom–atom–atom	angle, deg
C(1)–Pd(1)–P(1)	86.74(1)	C(27)–P(2)–Pd(1)	111.1(2)
C(1)–Pd(1)–P(2)	170.2(2)	C(21)–P(2)–Pd(1)	123.9(2)
P(1)–Pd(1)–P(2)	85.30(5)	C(20)–P(2)–Pd(1)	106.7
C(1)–Pd(1)–S(1)	93.5(2)	C(6)–C(1)–Pd(1)	124.5
P(1)–Pd(1)–S(1)	175.17(6)	C(2)–C(1)–Pd(1)	118.4
P(2)–Pd(1)–S(1)	93.99(5)	C(8)–C(7)–P(1)	121.0(5)
C(33)–S(1)–Pd(1)	114.5(2)	C(12)–C(7)–P(1)	120.4(5)
C(7)–P(1)–C(13)	104.9(3)	C(20)–C(19)–P(1)	109.1(4)
C(7)–P(1)–Pd(1)	118.7(2)	C(19)–C(20)–P(2)	109.1(4)
C(13)–P(1)–Pd(1)	114.7(2)	C(34)–C(33)–S(1)	121.5(4)
C(19)–P(1)–Pd(1)	107.2(2)	C(38)–C(33)–S(1)	120.9(5)
C(27)–P(2)–C(21)	104.7(3)		

that were suitable for analysis by X-ray diffraction; an ORTEP diagram is included in Figure 2. Data collection and refinement parameters and selected bond distances and angles are included in Tables 1, 4, and 5. The geometry about the Pd atom is planar; the Pd(1), S(1), P(1), and P(2) atoms lie within 0.0323 Å of the least squares plane. The P(1)–Pd(1)–P(2) bite angle in **24** is similar to that in **8** (85.30° vs 84.89° for **8**), while the C(1)–Pd(1)–S(1) bond angle is smaller (93.5° for **24** vs 95.7° for **8**). The palladium-bound aryl group is nearly orthogonal to the palladium square plane; the angle between the plane defined by Pd(1), S(1), P(1), and P(2) and the plane of the Pd-bound aryl group is 80.6°. The dihedral angle between the Pd-bound aryl group and the sulfur bound aryl group is 53°. The torsion angle defined by C(1), Pd(1), S(1), and C(33) is 26.7°, similar to the 28.2° torsional angle for alkyl thiolate **8**.

3. Palladium Alkylthiolato Complexes with Different Chelating Phosphines. Palladium thiolato aryl complexes and thiolato methyl complexes with different cis-chelating phosphine ligands were synthesized as summarized in eq 4. Complexes

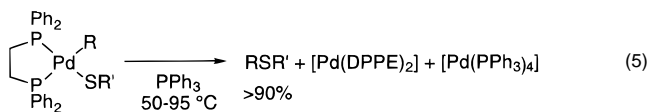


26–29 were formed in high yields from these reactions, but they formed fine powders and were isolated in unoptimized 14–

37% yields. An additional complex, [Pd(TRANSPHOS)(Me)-(S-*t*-Bu)] (**30**) with a trans-chelating phosphine, was synthesized by addition of the TRANSPHOS ligand to the thiolate dimer, [Pd(PPh₃)(Me)(S-*t*-Bu)]₂⁵² (TRANSPHOS = 2,11-bis(diphenylphosphinomethyl)benzo[*c*]phenanthrene). The displacement of PPh₃ by TRANSPHOS required heating at 85 °C for 7 h, as determined by monitoring the reaction by ¹H NMR spectroscopy. An analytically pure yellow crystalline solid was isolated in 88% yield. Complex **30** displayed a single resonance at δ 23.3 in the ³¹P{¹H} NMR spectrum, and the ¹H NMR spectrum showed two sets of inequivalent hydrogens corresponding to the methylene groups attached to the phosphorus atom.

B. Carbon–Sulfur Bond-Forming Reductive Elimination.

This paper describes a large number of reductive elimination reactions from organopalladium thiolato complexes. In all cases the yields of the reductive elimination reactions were high, as long as the reactions were conducted in the presence of a ligand to trap the Pd(0) fragment formed from the elimination process. When PPh₃ was used as the trap, the phosphorus-containing products at the end of the reductive elimination reaction were PdL₂ (L = chelating phosphine) and [Pd(PPh₃)₄]. In solution, Pd(PPh₃)₄ exists as a rapidly equilibrating combination of [Pd-(PPh₃)₃] and PPh₃.⁵³ This combination will be called PPh₃-ligated Pd(0) for the remainder of this paper. A general equation for the reductive elimination from DPPE-ligated complexes with PPh₃ as the trap is provided in eq 5. Kinetic and mechanistic



information is presented in section 1, and the detailed effects of the identity of the chelating phosphine, of the R and R' groups, and of the trapping ligand are discussed in section 2.

The reductive elimination reaction of complexes **1–12** and **14–15** to form Pd(0) completely consumed the thiolate starting material. However, the alkynyl complexes **16** and **17** were found to be in equilibrium with the mixture of Pd(0) species and the respective alkynyl *tert*-butyl sulfide. Approximately 5% of the starting thiolato complexes remained unreacted, and the same quantities of complexes **16** and **17** were generated by addition of the alkyl alkynyl sulfide to Pd(0). Prolonged heating converted both alkynyl *tert*-butyl sulfides to the di-*tert*-butyl sulfide, preventing detailed thermodynamic analysis. The fate of the alkynyl group was not determined.

The yield and rate of sulfide formation were dependent on the presence of a reagent to trap the Pd(0) fragment formed by aryl sulfide reductive elimination. The importance of the trapping ligand was studied most extensively for the *tert*-butylthiolato aryl complexes. In the absence of a reagent to trap [Pd(DPPE)], the sulfide product from the thermolysis of **1–12** was formed in only 45–65% yield (¹H NMR spectroscopy with internal standard). Addition of 2 or 10 equiv of triphenylphosphine, 10 equiv of diphenylacetylene, or 10 equiv of *p*-tolyl iodide as the trapping reagent gave greater than 95% yield of the desired sulfide and formed PPh₃-ligated Pd(0), the Pd(0) acetylene complex, or regenerated the aryl iodide complex, respectively.

1. Mechanism of Reductive Elimination of Sulfide. a. Kinetic Studies of Arylsulfide Reductive Elimination. Kinetic data for the reductive elimination of aryl *tert*-butyl sulfide from aryl *tert*-butylthiolato complexes **1–9** were obtained by

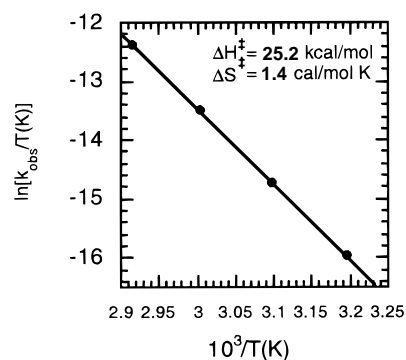


Figure 3. Eyring plot for the thermolysis of **2** in C₆D₆ over the temperature range 40–70 °C.

monitoring the disappearance of the palladium thiolato complexes in C₆D₆ by ¹H NMR spectroscopy. (Unless otherwise stated, the errors obtained for k_{obs} from kinetic runs were less than 5% of the value of k_{obs}.) In the presence of free PPh₃, plots of ln [Pd] vs time were linear over 3 half-lives for complexes **1–9**, demonstrating first-order dependence on the metal complex. The reactions showed a zero-order dependence on [PPh₃]. Observed rate constants for reactions conducted with a 6.0 mM concentration of complex **1** and concentrations of PPh₃ ranging from 30 to 240 mM were independent of [PPh₃]. An Eyring plot for the thermolysis of thiolato aryl complex **2** over the temperature range of 40–70 °C provided the activation parameters ΔH[‡] = 25.2 ± 0.2 kcal/mol ΔS[‡] = 1.4 ± 0.7 cal/(mol K) (Figure 3).

Addition of the potential radical inhibitors, dihydroanthracene or tri-*o*-tolylphosphine, in the absence of added PPh₃ gave similar products to reactions conducted without phosphine or radical trap. Quantitative rate studies were not conducted, but reactions run side by side showed no effect of these reagents on reaction rates in the presence or absence of added PPh₃. In addition, the observed rate constants for reactions conducted in THF and benzene were within a factor of 2. Observed rate constants for **2** in the presence of free PPh₃ at 50 °C in THF-d₈ and C₆D₆ were 8.2 × 10⁻⁵ and 1.3 × 10⁻⁴ s⁻¹, respectively.

To assess whether a portion of the chelating phosphine dissociated from the metal center during the reductive elimination process, reactions were studied involving alkylthiolato aryl complexes with chelating phosphines that have similar bite angles, but different flexibility in the backbone. Thermolysis of **2** and **26**, which have –CH₂CH₂– or 1,2-phenylene backbones, in the presence of free triphenylphosphine at 50 °C led to the formation of aryl alkyl sulfide, PdL₂ (L = chelating phosphine), and PPh₃-ligated Pd(0) in greater than 95% yield (¹H NMR spectroscopy with an internal standard). The rate of sulfide elimination was similar for both complexes. Reductive elimination from DPPE complex **2** showed a t_{1/2} of 96 min at 50 °C, while the DPPBz **26** showed a t_{1/2} value of 61 min at 50 °C.

Because the yield and rate of sulfide formation were different in the presence and absence of a ligand to trap the immediate Pd(0) product [Pd(DPPE)], the reaction rates were measured in the presence and absence of added ligand. The reaction rate was slower in the presence of a trap, but the yield of sulfide formation was higher (45–65% vs >95%). Thus, the rate of concurrent formation of side products is inhibited by the presence of PPh₃. The rate of reaction of phenyl complex **1** in the absence of a trap was 3.5 ± 0.5 × 10⁻⁴ s⁻¹, although the reaction deviated from first-order behavior after 2 half-lives. The rate of reaction of **1** in the presence of 10 equiv of PPh₃ was 2.4 ± 0.2 × 10⁻⁴, or 69% of that in the absence of a trap.

(52) Singhal, A.; Jain, V. K. *J. Organomet. Chem.* **1995**, *494*, 75–80.

(53) Amatore, C.; Pfluger, F. *Organometallics* **1990**, *9*, 2276–2282.

Reaction rates in the presence of phenylacetylene or *p*-tolyl iodide were within 20% of those measured with added phosphine. GC/MS analysis of the products from warming compounds **2–8** in the absence of trapping reagent revealed an exchange of the phosphine and palladium-bound aryl groups that occurred on a similar time scale to that of the reductive elimination reaction.^{54–58} For example, tolyl compound **2** yielded phenyl as well as *p*-tolyl *tert*-butyl sulfide product in a 1.3:1 ratio (65% overall yield) in the absence of a trap. In the presence of added trap, these products resulting from P–C cleavage were not observed.

b. Kinetic Studies of Alkyl Sulfide Reductive Elimination.

Because oxidative addition of alkyl and aryl halides can follow completely different mechanisms,^{53,59–64} it seemed possible that the reductive elimination of alkyl and aryl sulfides from methyl complex **14** and aryl complexes **1–9** could also follow different mechanisms. Further, it was important to compare the mechanisms of these two reactions to understand their relative rates discussed in detail below. Thus, the effect of the added dative ligand on reaction rate and yield along with the effect of solvent polarity, solvent hydrogen bonding ability, and added radical traps on reaction rate were evaluated for the formation of methyl *tert*-butyl sulfide from **14**.

Mechanistic results for complex **14** were similar to those for reductive elimination from arylthiolato complexes. Heating **14** with 2 or 10 equiv of PPh₃ gave greater than 90% yield of methyl *tert*-butyl sulfide, but reaction in the presence of 1 equiv of PPh₃ provided the sulfide in only 64% yield. Reductive elimination of **14** was first order in palladium complex through 3 half-lives in the presence of 2 equiv of PPh₃, and reaction rates for the thermolysis of 0.017 M of **14** in the presence of 0.08, 0.16, 0.25, and 0.33 M added PPh₃ were all within 8% of 2.0 × 10⁻⁵ s⁻¹, demonstrating a zero-order dependence on [PPh₃]. Complex **28**, which contains the more rigid chelating ligand DPPBz, underwent reductive elimination at a rate (2.2 × 10⁻⁵ s⁻¹ at 95 °C) that was nearly identical to that for DPPE-ligated **14**.

No significant rate differences were found when using benzene, THF, or *tert*-butyl alcohol as solvents. For example, reaction of **14** in the presence of free triphenylphosphine conducted in THF or *tert*-butyl alcohol had half-lives of 7 h at 95 °C compared to a half-life of 9.7 h when conducted in benzene. In the cases involving THF and *tert*-butyl alcohol, the half-lives were determined from the time of reaction to consume half of the starting complex, rather than from rate constants, but the qualitative results showed no significant solvent effect. No products from trapping the thyl radicals were observed by ¹¹B or ¹H NMR spectroscopy in reactions conducted in the presence of triethylborane.⁶⁵

(54) Goodson, F. E.; Wallow, T. I.; Novak, B. M. *J. Am. Chem. Soc.* **1997**, *119*, 12441–12453.

(55) Kong, K. C.; Cheng, C. H. *J. Am. Chem. Soc.* **1991**, *113*, 6313–6315.

(56) Herrmann, W. A.; Brossmer, C.; Priemeier, T.; Ofele, K. *J. Organomet. Chem.* **1994**, *481*, 97–108.

(57) Segelstein, B. E.; Butler, T. W.; Chenard, B. L. *J. Org. Chem.* **1995**, *60*, 12–13.

(58) Sakamoto, M.; Shimizu, I.; Yamamoto, A. *Chem. Lett.* **1996**, 1101–1102.

(59) Labinger, J. A.; Osborn, J. A. *Inorg. Chem.* **1980**, *19*, 3230–3236.

(60) Amatore, C.; Jutand, A.; Suarex, A. *J. Am. Chem. Soc.* **1993**, *115*, 9531–9541.

(61) Amatore, C.; Carre, E.; Jutand, A.; M'Barki, M. A. *Organometallics* **1995**, *14*, 1818–1826.

(62) Jensen, F. R.; Knickel, B. *J. Am. Chem. Soc.* **1971**, *93*, 6339–6340.

(63) Hartwig, J. F.; Paul, F. *J. Am. Chem. Soc.* **1995**, *117*, 5373–5374.

(64) Stille, J. K.; Lau, K. S. Y. *Acc. Chem. Res.* **1977**, *10*, 434–442.

(65) McPhee, D. J.; Campredon, M.; Lesage, M.; Griller, D. *J. Am. Chem. Soc.* **1989**, *111*, 7563–7567.

Table 6. Rates of Reductive Elimination for [Pd(DPPE)(R)(S-*t*-Bu)]

complex	R	temp, °C	<i>t</i> _{1/2} ^a min
14	methyl	95	580
15	alkenyl	50	17 ^b
1	phenyl	50	48
16	hexynyl	95	87
17	phenylethynyl	95	15 ^b

^a Unless noted otherwise, half-lives were determined from *k*_{obs} values, which were obtained by kinetic measurements over 3 half-lives. ^b Half-life was estimated from the time required to consume half of the starting complex.

Table 7. Rates of Reductive Elimination for Bis-Chelating Phosphines of [Pd(L)(Me)(S-*t*-Bu)]

complex	chelating ligand (L)	bite angle for [PdLCl ₂], ⁴⁸ deg	<i>t</i> _{1/2} ^a h
14	DPPE	85.8	10
27	DPPP	90.6	5
28	DPPBz		9 ^b
29	DPPF	99.1	0.5 ^c
30	TRANSPHOS	174.7	2 ^b

^a Reactions were conducted at 95 °C in sealed NMR tubes, and unless noted otherwise, half-lives were determined from *k*_{obs} values, which were obtained by kinetic measurements over 3 half-lives. ^b Half-life was estimated from the time of reaction to consume half of the starting complex. ^c This reaction was complete in less than 0.5 h.

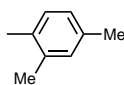
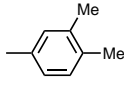
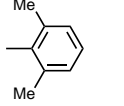
2. Reactivity Trends. a. Relative Rates for Reductive Elimination from Alkyl, Vinyl, Aryl, and Alkynyl *tert*-Butylthiolato Complexes. Carbon–sulfur bond-forming reductive elimination was observed directly from organopalladium thiolato complexes **1** and **14–16** containing alkyl, aryl, vinyl, or alkynyl groups bound to palladium. The half-lives for these reductive elimination reactions are given in Table 6. In most cases, rate constants were determined by monitoring the reactions run in the presence of trapping ligand over the course of 3 half-lives, and these *k*_{obs} were converted to *t*_{1/2}. From these data, the rates vary according to the trend alkenyl > aryl > alkynyl ≫ alkyl.

b. Effect of Ligand Bite Angle on Reaction Rates. The reductive elimination reaction was studied with complexes containing different P–M–P angles, commonly called “bite angles”. The rate of dialkyl sulfide reductive elimination was dramatically affected by this angle. Thermolysis of the DPPF-ligated *tert*-butylthiolato methyl complex **29** in the presence of free triphenylphosphine at 95 °C led to complete reductive elimination of alkyl sulfide and formation of phosphine-ligated Pd(0) species in less than 0.5 h. This rate was considerably faster than that for the corresponding DPPP complex **27** (*t*_{1/2} = 5 h at 95 °C), DPPBz complex **28** (*t*_{1/2} = 9 h at 95 °C), or DPPE complex **14** (*t*_{1/2} = 10 h at 95 °C) (Table 7). The yields of alkyl sulfide from the reductive elimination of complexes **14** and **27–29** were greater than 90%, as determined by ¹H NMR spectroscopy with an internal standard. In contrast to the stability of [Pd(TRANSPHOS)Me₂] reported previously,⁶⁶ the TRANSPHOS thiolato methyl complex **30** underwent reductive elimination of dialkyl sulfide in 77% yield in the presence of free triphenylphosphine after heating for 3.5 h at 95 °C.

c. Steric Effects on Sulfide Reductive Elimination. i. Effect of Thiolate Steric Properties. Reductive elimination of sulfide was studied for complexes with sterically distinct alkylthiolate ligands. Reductive elimination of alkyl sulfide from methyl methylthiolate complex **18** was markedly slower

(66) Morvskiy, A.; Stille, J. K. *J. Am. Chem. Soc.* **1981**, *103*, 2–4185.

Table 8. Rates of Reductive Elimination for Substituted [Pd(DPPE)(Ph)(SAr)]^a

complex	Ar	temp, °C	t _{1/2} , min
23		50	150
24		50	63
25		50	1500

^a Half-lives were estimated from the time of reaction required to consume half of the starting complex.

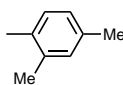
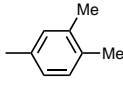
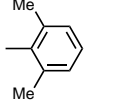
than reductive elimination from methyl *tert*-butylthiolate complex **14**. The reductive elimination from complex **14** had a t_{1/2} of 10 h at 95 °C, while no reaction occurred with complex **18** after heating in THF solvent in a sealed NMR tube submerged in a 95 °C water bath for more than 30 h. Similar results were observed for reactions conducted with alkylthiolato aryl complexes. The half-life at 50 °C for the reductive elimination of [Pd(DPPE)(C₆H₄-*p*-Cl)(S-*t*-Bu)] (**4**) was 1 h, in contrast to the 6 h half-life for the reductive elimination of [Pd(DPPE)(C₆H₄-*p*-Cl)(SCH₃)] (**13**) at 50 °C.

Reductive elimination was also studied for complexes with sterically distinct arenethiolate ligands, and the trends observed in this case contrasted those for alkylthiolates. Complexes **23**–**25** contain thiolate groups with 2,4-, 3,4-, and 2,6-dimethylphenyl substituents. The use of two methyl groups allowed us to alter the steric effects while minimizing electronic contributions. The half-lives for the reductive elimination of diaryl sulfide from **23**–**25** in the presence of free PPh₃ are given in Table 8. The reductive elimination was slowest for the most sterically hindered 2,6-dimethylphenyl thiolato complex **25** (t_{1/2} = 1500 min). Reductive elimination from the less hindered 2,4-dimethylphenyl thiolate **23** was faster (t_{1/2} = 150 min), and reductive elimination from the least sterically hindered 3,4-dimethyl arenethiolate complex **24** was the fastest (t_{1/2} = 63 min). Thus, the relative rates for reductive eliminations from complexes with arene thiolate ligands of varying size contrast the relative rates for reaction of complexes with alkyl thiolate ligands of varying size.

ii. Effect of Palladium-Bound Aryl Steric Properties. A series of substituted aryl *tert*-butylthiolate complexes were prepared to assess the trends in relative rates for reaction of complexes with sterically distinct palladium-bound aryl groups. These experiments were designed to probe coordination of the palladium-bound aryl group during the elimination reactions. Complexes **10**–**12** each contained aryl ligands bound to the palladium with two methyl groups substituted at different positions. Again, the use of two methyl groups allowed us to alter the steric effects while minimizing electronic contributions. The half-lives for the reductive elimination from **10**–**12** are given in Table 9. The rate for reaction of the 2,4-dimethylphenyl complex was slightly faster than that for the 3,4-dimethylphenyl complex. However, both rates were significantly faster than that for reductive elimination from 2,6-dimethylphenyl complex **12**, which required heating for over 100 h at 50 °C for half of the starting material to be consumed.

d. Electronic Effects on Reductive Elimination Reactions of Aryl and Alkyl Sulfides. i. Effect of Electronics on the

Table 9. Rates of Reductive Elimination for Substituted [Pd(DPPE)(Ar)(S-*t*-Bu)]^a

complex	Ar	temp, °C	t _{1/2} , min
10		50	41
11		50	55
12		50	6600

^a Half-lives were determined from k_{obs} values, which were obtained by kinetic measurements over 3 half-lives.

Table 10. Rate Constants, k_{obs} (s⁻¹ × 10⁴), as a Function of the Substituent, X, in [Pd(DPPE)(C₆H₄-X)(S-*t*-Bu)]

substituent (X)	k _{obs}	substituent (X)	k _{obs}	substituent (X)	k _{obs}
<i>p</i> -H	2.4	<i>m</i> -Me	2.3	<i>p</i> -NH ₂	0.36
<i>p</i> -Cl	1.1	<i>p</i> -OMe	0.33	<i>m</i> -NH ₂	2.5
<i>p</i> -Me	1.2	<i>m</i> -OMe	2.4	<i>p</i> -CF ₃	14

Pd-Bound Aryl Group. Table 10 shows the observed rate constants for reaction of complexes **1**–**9** and demonstrates that electron-donating substituents on the aryl group bound to the palladium have an overall decelerating effect on the reaction rate. The order of reaction rates for five of the para-substituted compounds was *p*-CF₃ > *p*-H > *p*-Me > *p*-OMe > *p*-NH₂ and showed the rough trend that donating groups decelerate the reaction, although *p*-Cl compound **4** underwent reductive elimination with a rate that was slower than that for reaction of the parent phenyl compound, despite the chloride substituent's small, positive σ -value. Hammett plots for the reductive elimination reactions from complexes **1**–**9** are shown in Figure 4. The plot on the top of Figure 4 shows that substituent effects in the formation of alkyl aryl sulfides from **1**–**9** do not follow a linear free energy relationship with the simple σ -values derived from benzoic acid acidity. Instead, a synthetic σ -value that is constructed from separate resonance and inductive parameters, with the resonance effect weighted more heavily than the inductive effect, provided the more linear relationship on the bottom of Figure 4. The treatment of these data parallels studies describing the separation of inductive and resonance effects in the reactions of organic compounds^{67,68} and provided the inductive and resonance ρ -values of $\rho_I = 1.7$ and $\rho_R = 5.0$.⁶⁹

ii. Effect of Electronics on the Arenethiolate. Reductive elimination reactions were conducted with the palladium aryl thiolate complexes **19**–**22** containing various substituents on the aryl ring bound to the sulfur atom of the thiolate ligand. The first-order rate constants for reductive elimination in the presence of 2 equiv of triphenylphosphine are provided in Table 11 and follow the trend in observed rate constants *p*-Cl < *p*-H < *p*-Me < *p*-OMe. Figure 5 shows a linear free energy relationship for these reductive eliminations. In this case, the slope is negative and shows that electron-rich thiolato ligands undergo C–S bond-forming reductive elimination faster than

(67) Ehrenson, S.; Brownlee, R. T. C.; Taft, R. W. *Prog. Phys. Org. Chem.* **1973**, *10*, 1–80.

(68) Wells, P. R.; Ehrenson, S.; Taft, R. W. *Prog. Phys. Org. Chem.* **1968**, *6*, 147–322.

(69) $\sigma = \sigma_I + \lambda_R / (1 + |\lambda|)$, where $\rho_I = \rho / (1 + |\lambda|)$ and $\rho_R = \rho \lambda / (1 + |\lambda|)$; ref 68, p 177 and references therein.

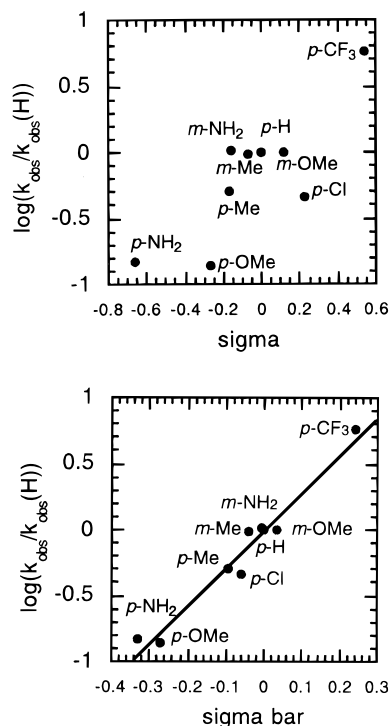


Figure 4. Free energy relationships for the C–S bond-forming reductive elimination reaction of **1–9**.

Table 11. Rate Constants, k_{obs} ($\text{s}^{-1} \times 10^4$), as a Function of the Substituent, X, in $[\text{Pd}(\text{DPPE})(\text{C}_6\text{H}_4\text{-}4\text{-}n\text{-Bu})(\text{S-C}_6\text{H}_4\text{-X})]$

substituent (X)	k_{obs}
<i>p</i> -Cl	1.3
<i>p</i> -H	4.3
<i>p</i> -Me	6.6
<i>p</i> -OMe	7.5

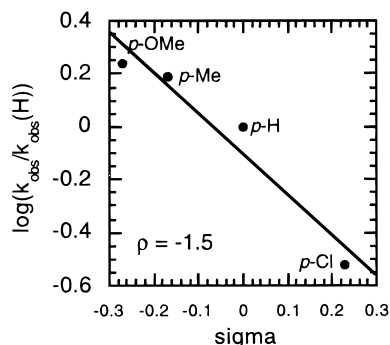


Figure 5. Free energy relationships for the C–S bond-forming reductive elimination reaction of **19–22**.

electron-poor thiolates. In addition, a linear relationship was observed with a standard σ -value in contrast to results in Figure 4. Fewer substituents were included in this portion of the electronic study, however.

Discussion

Potential Mechanisms for Sulfide Reductive Elimination.

There are several potential mechanisms for reductive elimination of sulfide from methyl, aryl, alkenyl, or alkynyl palladium thiolates. One mechanism involves initial dissociation of thiolate to generate an ion pair, while a second involves

generation of a thiyl radical. A third mechanism for reactions in the presence of aryl halide involves generation of a Pd(IV) intermediate, while reactions in the presence of phosphine could be initiated by coordination of phosphine to generate a five-coordinate complex. Finally, a single-step reductive elimination from Pd(II) could occur directly from the isolated four-coordinate complex or from a species generated by phosphine dissociation, which would be ligand dechelation in this case. Carbon–carbon bond-forming reductive elimination reactions have been shown to occur from 5-coordinate species in nickel systems, from 3-coordinate species in Pd(II) systems,⁶⁶ and after initial reaction of alkyl iodides with some Pd(II) species.⁷¹

Mechanism of Aryl Sulfide Reductive Elimination. The reductive elimination of aryl sulfides in our system was zero order in trapping reagent, including aryl iodide, ruling out both an association of the phosphine followed by reductive elimination from a 5-coordinate intermediate and the formation of a Pd(IV) intermediate that eliminates sulfide. Reaction rates were clearly independent of phosphine concentration, and there was no evidence for the buildup of a five-coordinate species. Potential reaction from a three-coordinate complex is more difficult to probe, and elimination after dechelation cannot be deduced from rate behavior in added ligand. However, complex **26** containing a rigid and preorganized chelating backbone did not react slower than that containing DPPE as would be expected if dechelation occurred prior to reductive elimination. Although this observation does not rigorously rule out phosphine dissociation that would reversibly open the chelate ring before reductive elimination from a three-coordinate species, these data strongly suggest carbon–sulfur bond-forming reductive elimination occurs in these systems directly from the isolated four-coordinate complex. Related reductive elimination of arylamine from a four-coordinate PPh_3 -ligated complex has been detected recently by kinetic studies, and elimination of arylamine has been observed from DPPF-ligated palladium amido aryl complexes.^{9,14,16}

Mechanism of Dialkyl Sulfide Reductive Elimination.

Mechanistic studies were conducted with *tert*-butylthiolate methyl complex **14** to determine whether the difference in reaction rates between elimination from aryl complex **1** and alkyl complex **14** noted in the Results section could be explained by a dramatic change in mechanism. Since the reactions of **14** showed no significant difference in rate when conducted in polar protic, polar aprotic, or nonpolar solvents, one can rule out an ionic mechanism, such as one involving thiolate dissociation and attack on the palladium methyl. One can also argue strongly against a mechanism involving thiyl radicals due to the absence of products resulting from thiyl radical trapping by triethylborane. Triethylborane reacts with *tert*-butyl thiyl radicals to form diethyl-*tert*-butyl thiolato borane with a rate constant of $1.3 \times 10^8 \text{ M}^{-1} \text{ s}^{-1}$.

The zero-order dependence of the rate on phosphine concentration rules out a mechanism involving association of a phosphine to form a 5-coordinate intermediate. The similar rates for reactions of **28**, which contains the more rigid chelating ligand DPPBz, and of **14**, which contains DPPE, argue against a mechanism in which one arm of the phosphine dissociates to form a three-coordinate intermediate. In summary, the reductive elimination involving a saturated methyl group most likely proceeds by an intramolecular, concerted mechanism analogous to that for the reductive elimination of sulfide from complexes containing palladium-bound aryl groups.

(70) Tatsumi, K.; Nakamura, A.; Komiya, S.; Yamamoto, A.; Yamamoto, T. *J. Am. Chem. Soc.* **1984**, *106*, 1–8188.

(71) Ozawa, F.; Yamamoto, A. *Chem. Soc. Jpn.* **1987**, *5*, 773–784.

Effect of Trapping Reagent on Reaction Rate and Yield.

The presence of a trapping reagent greatly affected the yield and rate of sulfide formation. It is possible that phosphine concentration could affect the selectivity of a common intermediate that forms all of the products, or that added ligand could accelerate reductive elimination of sulfide. Alternatively, different rate determining steps could form the sulfide and the side products, and the steps that form side products could be inhibited by added phosphine, leading to increased reaction yields in the presence of PPh_3 . The first possibility would provide the same reaction rate in the presence or absence of a trap, and the second possibility would give faster rates in the presence of a trap. These predictions are both inconsistent with the slightly faster reaction rates in the absence of a trap and the zero-order behavior in the trapping ligand when enough trap is present to produce a stable palladium product. Thus, the trapping reagents inhibit reaction pathways other than the desired sulfide elimination reaction and account for the improved yields in the presence of phosphine, acetylene, or aryl halide.

The side products formed from reactions conducted without trapping ligand included organic biaryl compounds. These products included aryl groups from the phosphine, as well as the one bound to palladium. The mechanism for aryl exchange is not clear at this point, but similar aryl exchange behavior was observed for reactions containing radical traps such as dihydroanthracene or tri-*o*-tolylphosphine instead of PPh_3 . These data argue against a competing decomposition through a radical intermediate. We suggest that the ill-defined Pd(0) products formed in the absence of a trap induce the formation of the various biaryl products. Studies on the mechanism of P–C bond cleavage do not provide straightforward conclusions;^{54,55,72} whatever the mechanism, it is important that added trapping reagent shuts down this exchange process and allows clean formation of substituted aryl sulfides.

Effect of Chelating Ligand on Reaction Rate. Methods to increase reaction rates and yields by perturbing ligand structure may lead to improved catalysts for hetero cross-coupling processes. The differences in observed rate constants for reaction of complexes **14** and **27–29** show that increasing the P–Pd–P angle facilitates reductive elimination of sulfide. This effect has been noted in studies of stoichiometric C–C bond-forming reductive eliminations from Pd(II), and complexes containing ligands with large bite angles undergo fast C–C bond-forming reductive eliminations.⁷³ Appropriate ligand bite angle may also account for the success of DPPF-ligated palladium complexes in the catalytic amination of aryl halides.^{10,28}

Increasing reductive elimination rate with increasing bite angle may be caused by a large bite angle forcing the two covalent ligands of a square-planar four-coordinate complex to become closer together, thereby creating a ground state that is closer in structure to the transition state and a faster reductive elimination.^{74–76} A survey of four-coordinate bis-chelating phosphine dichloride complexes prepared previously showed that increasing the size of the bite angle decreases the angle between the two chloride ligands. For example, the P–Pd–P angle in $[\text{Pd}(\text{DPPE})\text{Cl}_2]$ is 13.3° smaller than that in $[\text{Pd}(\text{DPPF})\text{Cl}_2]$ (85.8° vs 99.1°), and the Cl–Pd–Cl angle is larger by 6.4°

(from 94.2° to 87.8°).⁴⁸ Although not an isosteric comparison, the bite angle in **24** is larger than that in $[\text{Pd}(\text{DPPF})(\text{Ar})(\text{NtoI}_2)]^9$ by 15° , while the C–Pd–S angle in **24** is 8° smaller than the C–Pd–N angle in $[\text{Pd}(\text{DPPF})(\text{Ar})(\text{NtoI}_2)]$.

Alternatively, the effect of bite angle on elimination rates can be rationalized by a P–Pd–P angle in the initial Pd(0) product that is closer to the preferred linear geometry of an $\text{L}_2\text{-Pd}(0)$ complex.^{48,73,77} The product of the elementary reductive elimination step would be more stable, making the transition state lower in energy by the Hammond postulate. Structurally, the transition state for reductive elimination would be most stable with a large bite angle. Thus, the transition state would have less strain in the metal–phosphine ligand ring system for complexes with large bite angles.

We were surprised to discover that complex **30** with its trans-chelating ligand, TRANSPOS, underwent reductive elimination to form alkyl sulfide. The mechanism of C–C bond-forming reductive elimination from 4-coordinated palladium complexes is believed to occur exclusively from complexes with a cis geometry, a conclusion that is supported by the resistance of $[\text{Pd}(\text{TRANSPOS})(\text{Me})_2]$ to undergo reductive elimination of ethane.⁶⁶ In contrast, the $[\text{Pd}(\text{TRANSPOS})(\text{Me})(\text{S}-t\text{-Bu})]$ complex **30** underwent facile reductive elimination in a nonpolar solvent. According to the Cambridge Structural Data Base, there are two crystal structures of group 8 TRANSPOS complexes: $[\text{Pd}(\text{TRANSPOS})(\text{Cl})_2]$ and $[\text{Pt}(\text{TRANSPOS})(\text{Cl})_2]$. The P–Pd–P and Cl–Pd–Cl bond angles of the Pd dichloride complex are 174.7 and 168.3° , but the P–Pt–P and Cl–Pt–Cl angles for the Pt dichloride complex are an unexpected 104.8 and 87.1° , respectively.^{78,79}

In other words, $[\text{Pt}(\text{TRANSPOS})(\text{Cl})_2]$ is a cis-mononuclear complex, and the energies of the cis and trans forms of TRANSPOS complexes are, in fact, similar. The greater size of the *tert*-butyl thiolato ligand, relative to a methyl ligand, may lead to more rapid dissociation of one arm of the TRANSPOS ligand. This dechelation could lead to either reductive elimination from a three-coordinate complex or isomerization of the TRANSPOS complex to generate a highly reactive cis complex. Alternatively, the π -donating ability of the sulfur may accelerate the partial dissociation, again leading to reductive elimination from a three-coordinate species or isomerization to the cis complex. Reductive elimination from a four-coordinate cis “TRANSPOS” complex would be fast because of the extremely large bite angle of this ligand and the more stable linear Pd(0) product.

Potential Mechanisms for Elimination from Four-Coordinate Pd(II) Complexes. Although difficult to answer unambiguously, one can address more detailed questions about the intimate mechanism for reductive elimination from the four-coordinate Pd(II) complex. Two classes of mechanisms can be envisioned. The reductive elimination could occur by synchronous coupling of the aryl and thiolate ligands such as the elimination of ethane from a dimethyl complex,⁶⁶ or it could occur by migration of one ligand to the other. This latter mechanism could involve either migration of the hydrocarbyl group as an electrophile (Scheme 1) or nucleophilic attack of the thiolate on the aryl group (Scheme 2). These mechanisms are similar to that calculated for P–C cleavages in phosphine ligands.⁸⁰ As we address the consistency of these mechanisms

(72) Morita, D. K.; Stille, J. K.; Norton, J. R. *J. Am. Chem. Soc.* **1995**, *117*, 8576–8581.

(73) Brown, J. M.; Guiry, P. J. *Inorg. Chim. Acta* **1994**, *220*, 249–259.

(74) Kohara, T.; Yamamoto, T.; Yamamoto, A. *J. Organomet. Chem.* **1980**, *192*, 265–281.

(75) Steffen, W. L.; Palenik, G. J. *Inorg. Chem.* **1976**, *15*, 2432–2442.

(76) Gramlich, V.; Consiglio, G. *Helv. Chim. Acta* **1979**, *62*, 1016–1024.

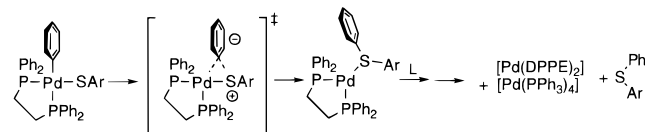
(77) Steffen, W. L.; Palenik, G. J. *Inorg. Chem.* **1976**, *15*, 2432–2439.

(78) Bracher, G.; Grove, D. M.; Venanzi, L. M.; Bachechi, F.; Mura, P.; Zambonelli, L. *Helv. Chim. Acta* **1980**, *63*, 2519–2530.

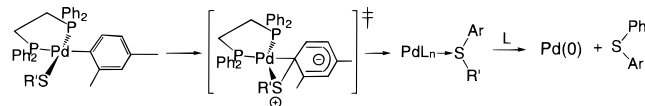
(79) Bachechi, F.; Zambonelli, L. *Acta Crystallogr., C* **1992**, *48*, 788–792.

(80) Ortiz, J. V.; Havlas, Z.; Hoffmann, R. *Helv. Chim. Acta* **1984**, *67*, 1–17.

Scheme 1



Scheme 2



with experimental data, we also address the potential for coordination of the hydrocarbyl group to palladium during the transition state. Such coordination has been used previously to explain relative rate data.^{5–8} In all cases, reductive elimination must occur from the four-coordinate Pd(II) complex with both portions of the chelating phosphine bound to the metal, as is required by our mechanistic data.

Relationship of the Hydrocarbyl Ligand and the Rate of Reductive Elimination. The thermal chemistry displayed by the alkyl complex **14**, alkenyl complex **15**, phenyl complex **1**, and alkynyl complex **16** in these systems indicates that unsaturated ligands have a greater propensity to participate in reductive elimination than saturated alkyl groups. Although the general mechanistic features of RS-*t*-Bu reductive elimination involving saturated and unsaturated R groups are similar, intimate factors must exist that significantly influence reductive elimination rates. Clearly, the data presented so far do not support a smooth relationship between reaction rate and hybridization. For example, reaction rates dictated by metal–ligand bond strengths would follow the order $sp^3 > sp^2 > sp$. Reaction rates dictated by formation of a stronger carbon–sulfur bond would follow in the order $sp > sp^2 > sp^3$. Rates dictated by ligand basicity would follow the order $sp > sp^2 > sp^3$, or vice versa depending on whether a more or less basic ligand reacts faster. Finally, if the stability of the starting thiolate complexes were strongly influenced by steric factors, then the rates should follow in the order $sp^3 > sp^2 > sp$ or $sp^2 > sp^3 > sp$. None of these predicted trends were observed. Without knowledge of accurate metal–ligand and carbon–sulfur bond strengths, it is difficult to ascertain whether the relative rates are a result of thermodynamic or kinetic factors. However, we suggest that simple coupling of the two covalent ligands without involvement of the π -systems is unlikely to be occurring.

Instead, a migration mechanism that involves the π -system of the hydrocarbyl group and possibly coordination of this π -system to the metal center is more likely. Alkene complexes are common and arene complexes are also known.⁸¹ Thus, coordination of these π -systems to the metal during the reaction may stabilize the transition state. Further, theoretical calculations predict that migration of the hydrocarbyl ligand is more rapid for unsaturated ligands.^{80,82} This effect would explain the faster rates for reductive elimination from alkenyl, aryl, and alkynyl complexes than from the alkyl complexes.

The relative rates of elimination from the alkynyl vs. alkenyl and aryl complexes are more difficult to rationalize. We suggest two explanations. In the first, coordination of the hydrocarbyl group to the metal center is again used to rationalize the relative

rates. One might expect the more stable coordination of alkynes, relative to that of alkenes or arenes, to provide faster rates for formation of alkynyl sulfides if the relative rates are to be explained by π -coordination in the transition state for reductive elimination. However, the distortion required for the alkynyl ligand to coordinate via the π -system may attenuate the energetic benefit from the coordination. The energetic penalty for this distortion may be small because the energy for deformation of acetylenic compounds from linearity in organic systems is modest.⁸³ However, the difference in activation energies for elimination from the alkynyl compounds and the aryl or vinyl compounds is on the order of only 4–5 kcal/mol, which may be similar to this deformation energy.

We also provide an alternative explanation based on ground state energetics. The slower elimination from the alkynyl complex compared to the alkenyl and aryl complex could simply be justified by the smaller thermodynamic driving force for this reaction. As presented in the Results section, the alkynyl palladium thiolate complex equilibrates with observable quantities of the Pd(0) products and the alkynyl sulfide. Thus, the complexes with unsaturated ligands would eliminate faster than the methyl complex for reasons of π -coordination in the transition state, but the complex with the alkynyl ligand would eliminate more slowly than those with other unsaturated ligands due to less favorable thermodynamics.

Electronic Effects. Decreasing electron density at the metal often accelerates reductive elimination, and this general observation would predict that increasing the donating ability of the aryl and thiolate groups would decrease the rates for reductive elimination. In contrast, theoretical work has shown that more weakly donating dative ligands, but more donating covalent ligands would accelerate reductive elimination from Pd(II).⁸⁴ Thus, our general result that more nucleophilic sulfide ligands and more electrophilic aryl ligands lead to the fastest elimination rates cannot be explained by conventional arguments based on overall metal electron density, or arguments made in theoretical work based on changes in metal d-orbital energies during reductive elimination. Instead, electron-rich thiolate ligands and electron-poor aryl ligands led to faster rates.⁹ These electronic effects again disfavor a synchronous coupling of the two groups. They instead favor a mechanism involving intramolecular attack of the thiolate ligand as a nucleophile on an electrophilic hydrocarbyl group.

The electronic effects in our study were complex. The analysis of electronic effects based on σ_{R^-} and σ_I values showed that resonance effects dominated inductive effects in determining reaction rates. The larger ρ_{R^-} value for the resonance contribution indicates that the transition state is more greatly affected by substituents that are conjugated with the aryl ring. Similar electronic effects were observed with the different alkynyl complexes. Reductive elimination from phenyl ethynyl complex **5** was faster than that from hexynyl complex **4**. The electron-withdrawing nature of the phenyl group on the alkynyl ligand led to faster reductive elimination. In contrast to faster rates for electron-poor aryl groups, reaction rates were faster for electron-rich thiolates, and an acceptable linear relationship between $\log k$ and a standard σ was observed. Similar cooperative electronic effects on the reactivity of platinum diaryl complexes has been observed qualitatively. Pt(II) complexes with two electron-rich or two electron-poor aryl groups were stable, but complexes with one electron-rich and one electron-

(81) Collman, T. P.; Hegedus, L. S.; Norton, J. R.; Finke, R. G. *Principles and Applications of Organotransition Metal Chemistry*, 2nd ed.; University Science Books: Mill Valley, CA, 1987; pp 161–163.

(82) Calhorda, M. J.; Brown, J. M.; Cooley, N. A. *Organometallics* **1991**, *10*, 1431–1438.

(83) Viola, A.; Collins, J. J.; Filipp, N. *Tetrahedron* **1981**, *37*, 3765–3811.

(84) Tatsumi, K.; Hoffmann, R.; Yamamoto, A.; Stille, J. K. *Bull. Chem. Soc. Jpn.* **1981**, *54*, 7–1867.

poor aryl group could not be isolated.⁸⁵ A similar dominance of resonance electronic effects has been observed with C–O and C–N bond-forming reductive elimination^{12,13,16,50} and in catalytic formation of ethers and amines.^{12,13,16} Therefore, the large resonance effect on the rate of reductive elimination involving Pd(II) aryl complexes appears to be general.

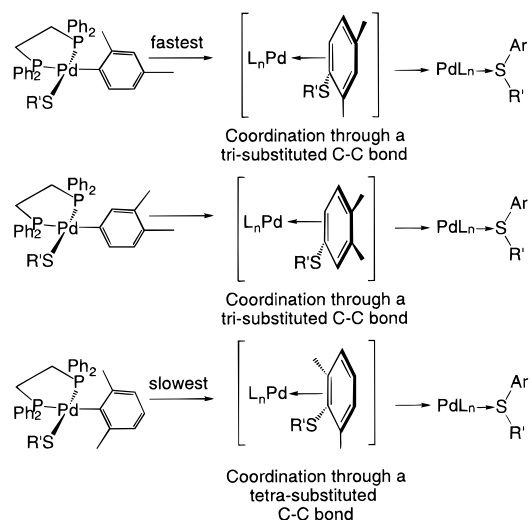
The importance of resonance effects is again consistent with a mechanism involving migration of the thiolate to the hydrocarbyl ligand or vice versa, concomitant with coordination of the π -system of the hydrocarbyl ligand. In a migration mechanism, the hydrocarbyl group π -system would bridge the metal and the thiolate sulfur. However, this mechanism does not explain the large ρ_R . This intermediate resembles the Meisenheimer intermediate in S_NAr reactions, and S_NAr reactions do not have larger ρ_R than ρ_I .⁶⁷ Alternatively, coordination of the hydrocarbyl group π -system could occur in conjunction with nucleophilic attack by the thiolate. This coordination could help the aromatic system to absorb the increase in electron density. The coordination of ligands to transition metals as π -complexes is greatly affected by the HOMO–LUMO gap, and therefore coordination of the aryl π -system could generate a large resonance substituent effect.

It should be noted that the ρ -values were modest. The absence of a measurable solvent effect is consistent with these modest ρ -values. These data indicate that a large charge buildup is not occurring in the transition state, although solvent effects are typically less pronounced for reactions with organometallic compounds than for purely organic molecules.⁸⁶ The magnitude of these ρ -values is crucial to the generality of the reductive elimination chemistry and to synthetic applications. The ρ -values are smaller than those for direct nucleophilic aromatic substitution reactions, including studies on S_NAr reactions with arene thiolate nucleophiles. Thus, the small ρ -values make cross-coupling reactions involving carbon–heteroatom bond-forming reductive eliminations more general than direct, uncatalyzed S_NAr reactions.

Steric Effects. The steric effects of the palladium-bound aryl group (Table 9) on reaction rate are not readily explained by a simple synchronous coupling or migration mechanism. Instead, C–S bond-forming reductive elimination that involves coordination of the hydrocarbyl group allows one to explain the unusual steric effects. Scheme 3 shows how coordination may be occurring for a mechanism involving complexes with palladium-bound aryl groups. The aryl group is coordinated to the metal center through a multiple C–C bond to form a 16-electron metal complex. The mono-ortho-substituted system would coordinate to the metal through a trisubstituted C–C bond, while the di-ortho-substituted system would gain less stability by coordination to the metal because coordination is limited to a tetrasubstituted C–C bond. Reductive elimination from the 2,4-dimethyl complex would be faster than that from the 3,4-dimethyl complex because of decreasing steric effects from the ground state for the 2,4-dimethyl complex. These predictions are, indeed, the trends in reaction rates. Thus, we propose that coordination of the hydrocarbyl group is involved in the transition state structure for a migration mechanism.

Steric Effects of Thiolate Substituents. The steric effects of the thiolate substituents on reaction rate were unusual. An increase in the size of alkyl groups increased reaction rates but

Scheme 3



an increase in the size of aryl groups decreased reaction rates (Table 8). Effects of steric properties on the alkyl thiolate ligand can be explained in a simple manner by the premise that larger thiolates will lead to faster reductive elimination as a result of a greater decrease in steric hindrance from the starting material as the metal–ligand bonds lengthen in the transition state for elimination. Further, these results imply that coordination through the sulfur atom does not control reaction rates. If coordination through sulfur were important in dictating reaction rates, then elimination from the methylthiolate complex would be faster than that from the *tert*-butylthiolate complex because the intermediate sulfide complex formed from the methylthiolate would be less hindered and, therefore, more stable than that formed from the *tert*-butylthiolate.

It was unexpected that increasing the steric properties of aryl thiolates would provide the opposite effect to that observed with alkyl thiolates. The crystal structure of alkylthiolate complex **8** and arylthiolate complex **24** shows little difference in ground-state structural features such as Pd–S–R angle or dihedral angle between the palladium square plane and palladium-bound aryl group plane. Therefore, explanations for relative rate trends cannot be based on ground-state geometry. Thus, steric interactions in the transition state of the aryl thiolate eliminations must increase, rather than decrease, relative to those in the ground state, and the structural differences lie in the transition state. A difference in transition state structures may result from stereoelectronic effects. An electronic interaction present in the aryl thiolate complexes may provide a geometry that has more steric congestion than the ground state, such as one with the aryl group lying in the metal square plane to maximize overlap with a sulfur electron pair.

It is difficult to provide a definitive conclusion about which intimate mechanisms are occurring, but we hope that this discussion provides working models for how structural and electronic perturbations on the systems can affect relative rates for C–X bond-forming reductive eliminations. These experimental studies also provide guidance on the reaction rates of the C–X coupling step in catalytic processes such as aryl halide thiation, etherification, and amination reactions. It seems that computational studies on these C–S bond-forming reductive eliminations and related C–N and C–O bond-forming reductive eliminations would help to select between or refine our proposed intimate mechanisms.

(85) Brune, H. A.; Strapp, B.; Schmidtberg, G. *J. Organomet. Chem.* **1986**, *307*, 129–137.

(86) MeI is known to oxidatively add to Vaska's complex by an S_N2 mechanism, but the solvent effects for the oxidative addition of MeI to Vaska are much smaller than that for an organic S_N2 reaction. Chock, P. B.; Halpern, J. *J. Am. Chem. Soc.* **1966**, *88*, 3511–3514.

Conclusions

Carbon–sulfur bond-forming reductive elimination from saturated and unsaturated hydrocarbyl ligands occurs from a 4-coordinate palladium thiolato complex. The reductive elimination reaction is facilitated by palladium complexes with large bite angles, electron-deficient carbon-bound ligands, and electron-rich thiolato ligands. The relative rates of reductive elimination were fastest from complexes with alkenyl and aryl ligands, slower from complexes with alkynyl ligands, and significantly slower from complexes with alkyl ligands. These trends can best be explained by kinetic rather than thermodynamic factors in which coordination of the π -system of an unsaturated covalent ligand stabilizes the reductive elimination transition state.

Experimental Section

General Methods. All reactions were performed in a drybox or with Schlenk techniques under N_2 . 1H and $^{13}C\{^1H\}$ NMR spectra were obtained on a QE 300 MHz spectrometer. Chemical shifts were referenced to residual protiated solvents. $^{31}P\{^1H\}$ NMR spectra were obtained on an Omega 300 MHz spectrometer with shifts reported relative to an external 85% H_3PO_4 standard. For $^{31}P\{^1H\}$ NMR spectra, a downfield chemical shift is considered positive. Satisfactory elemental analyses were obtained for all complexes except **1**, **3**, **6**, **9**, **15**, **24**, and **29**. Elemental analysis was performed by MicroAtlantic Lab, Ind. in Norcross, Ga. IR spectra were recorded on a MIDAC Fourier Transform spectrometer. GC/MS data were obtained on an HP 5890 gas chromatograph equipped with an HP5971A mass spectral analyzer.

General Procedure for the Synthesis of $[Pd(L)(R)(X)]$, Where L = Bisphosphine, R = Hydrocarbyl Group, and X = Halide. Except in cases where R = Me, reaction of 1.5 equiv of RX and $[Pd(PPh_3)_4]$ in benzene resulted in the formation of $[Pd(PPh_3)_2(R)(X)]$, which was isolated by precipitation from pentane and was used without further purification. Reaction of a bis-chelating phosphine, L, and $[Pd(PPh_3)_2(R)(X)]$ in benzene resulted in the formation of $[Pd(L)(R)(X)]$, which was isolated by precipitation from pentane and used without further purification. $[Pd(L)(Me)(X)]$ was synthesized by reaction of $[(COD)Pd(Me)Cl]^{49}$ and a bisphosphine, L. The $^{31}P\{^1H\}$ spectra for $[Pd(L)(R)(X)]$ are as follows: $[Pd(DPPE)(Ph)(I)]$ (THF) 48.9 (d, 28 Hz), 33.9 (d, 28 Hz); $[Pd(DPPE)(C_6H_4-4-Me)(I)]$ (THF) 48.7 (23.2 Hz), 34.1 (broad); $[Pd(DPPE)(C_6H_4-3-Me)(I)]$ (THF) 49.0 (d, 24 Hz), 33.5 (d, 24 Hz); $[Pd(DPPE)(C_6H_4-4-Cl)(I)]$ (THF) 50.5 (d, 25 Hz), 36.3 (d, 25 Hz); $[Pd(DPPE)(C_6H_4-4-OMe)(I)]$ (THF) 49.2 (d, 26 Hz), 33.5 (d, 26 Hz); $[Pd(DPPE)(C_6H_4-3-OMe)(I)]$ (THF) 51.5 (d, 26 Hz), 36.3 (d, 26 Hz); $[Pd(DPPE)(C_6H_4-4-NH_2)(I)]$ (CH_2Cl_2) 47.19 (d, 25.64 Hz), 32.71 (d, 25.64 Hz); $[Pd(DPPE)(C_6H_4-3-NH_2)(Br)]$ (THF) 49.9 (broad), 30.0 (broad); $[Pd(DPPE)(C_6H_4-4-CF_3)(Br)]$ (THF) 52.2 (d, 25 Hz), 32.3 (d, 25 Hz); $[Pd(DPPE)(2,4-(CH_3)_2C_6H_3)(I)]$ (C_6H_6) 45.2 (d, 26 Hz), 30.8 (d, 26 Hz); $[Pd(DPPE)(3,4-(CH_3)_2C_6H_3)(I)]$ (C_6H_6) 48.5 (d, 27 Hz), 33.1 (d, 27 Hz); $[Pd(DPPE)(2,6-(CH_3)_2C_6H_3)(I)]$ (C_6H_6) 46.7 (d, 29 Hz), 24.9 (d, 29 Hz); $[Pd(DPPE)(Me)(Cl)]$ (THF) 59.7 (d, 27 Hz), 32.0 (d, 27 Hz); $[Pd(DPPE)(CC(CH_3)_3CH_3)(I)]$ (THF) 54.6 (d, 8 Hz), 47.6 (d, 8 Hz); *trans*- $[Pd(PPh_3)_2(CCC_6H_5)(Br)]$ (THF) 25.5 (s); $[Pd(DPPBz)(C_6H_4-4-Me)(I)]$ (THF) 50.5 (d, 27 Hz), 43.4 (d, 27 Hz); $[Pd(DPPEE)(C_6H_4-4-Me)(I)]$ (THF) 55.5 (d, 13.4 Hz), 48.0 (d, 13.4 Hz); $[Pd(DPPP)(Me)(Cl)]$ (THF) 26.8 (d, 48.9 Hz), -7.1 (d, 48.9 Hz); *trans*- $[Pd(PPh_3)_2(Me)(Cl)]$ (THF) 31.17 (s); $[Pd(DPPF)(Me)(Cl)]$ (THF) 37.7 (d, 32 Hz), 11.2 (d, 32 Hz); *trans*- $[Pd(PPh_3)_2(C_6H_4-n-Bu)(I)]$ (THF) 24.12 (s).

Representative Procedures. Complete syntheses and elemental analysis data are provided in the Supporting Information.

$[Pd(Ph_2PCH_2CH_2PPh_2)(S-t-Bu)(Ph)]$ (1**).** To a 20 mL vial was added 89.5 mg (0.126 mmol) of $[Pd(DPPE)(Ph)(I)]$ and 19.1 mg (0.171 mmol) of 2-methyl-2-propanethiol, sodium salt as solids. The mixture was suspended in 10 mL of THF and stirred at room temperature for 20 min after which time the THF was removed under vacuum. The residual solid was dissolved in benzene and filtered through Celite to remove residual salts. The benzene was then removed under vacuum and the product was obtained in 34.6 mg (40.9%) as a green crystalline solid by slow diffusion of ether into a THF solution of the product. 1H

NMR (C_6D_6) δ 1.62 (s, 9H), 1.74–1.92 (m, 4H), 6.85–7.00 (m, 8H), 7.01–7.26 (m, 11H), 7.70 (t, 7.3 Hz, 2H), 8.10 (t, 8.8 Hz, 4H); $^{31}P\{^1H\}$ NMR (C_6D_6) δ 32.4 (d, 25 Hz), 42.6 (d, 25 Hz); IR (KBr, cm^{-1}) 3044 (m), 2966 (m), 2940 (m), 2909 (m), 2880 (m), 1559 (s), 1434 (s), 1153 (m), 1102 (s), 1014 (s), 690 (vs).

$[Pd(Ph_2PCH_2CH_2PPh_2)(S-t-Bu)(C_6H_4-4-Me)]$ (2**).** The product was obtained in 33.5% (34.9 mg) yield after crystallization by layering a ether solution with pentane at $-35^\circ C$. 1H NMR (C_6D_6) δ 1.60 (s, 9H), 1.60–1.92 (m, 4H), 2.08 (s, 3H), 6.73–6.99 (m, 2H), 7.00–7.23 (m, 16H), 7.53 (t, 7.5 Hz, 2H), 8.06 (m, 4H); $^{31}P\{^1H\}$ NMR (C_6D_6) δ 32.7 (d, 24 Hz), 42.9 (d, 24 Hz); IR (KBr, cm^{-1}) 3045 (m), 3005 (m), 2942 (m), 2909 (m), 2877 (m), 2850 (m), 1585 (m), 1479 (m), 1433 (s), 1155 (s), 1100 (s), 1013 (s), 789 (s), 693 (vs).

$[Pd(Ph_2PCH_2CH_2PPh_2)(S-t-Bu)(C_6H_4-3-Me)]$ (3**).** The product was obtained in 55.9% (77.7 mg) yield after crystallization by layering a ether solution with pentane at $-35^\circ C$. 1H NMR (C_6D_6) δ 1.65 (s, 9H), 1.65–1.99 (m, 4H), 2.04 (s, 3H), 6.70 (d, 7.3 Hz, 1H), 6.93 (m, 9H), 7.00–7.26 (m, 8H), 7.36 (d, 6.3 Hz, 1H), 7.62 (t, 6.3 Hz, 4H), 8.11 (t, 8.1 Hz, 4H); $^{31}P\{^1H\}$ NMR (C_6D_6) δ 31.44 (d, 25.6 Hz), 42.45 (d, 25.6 Hz).

$[Pd(Ph_2PCH_2CH_2PPh_2)(S-t-Bu)(C_6H_4-4-Cl)]$ (4**).** The product was obtained in 61.7% (86.7 mg) yield after crystallization by layering a toluene solution with pentane at $-35^\circ C$. 1H NMR (C_6D_6) δ 1.55 (s, 9H), 1.65–1.95 (m, 4H), 6.85–6.99 (m, 2H), 7.00–7.21 (m, 16H), 7.39 (t, 7.5 Hz, 2H), 7.49 (t, 7.5 Hz, 2H), 8.06 (t, 8.7 Hz, 4H); $^{31}P\{^1H\}$ NMR (C_6D_6) δ 33.85 (d, 24.2 Hz), 43.59 (d, 24.2 Hz); IR (KBr, cm^{-1}) 3050 (m), 2928 (m), 2910 (m), 2855 (m), 1481 (m), 1463 (m), 1434 (s), 1151 (s), 1102 (s), 1082 (s), 1003 (s), 803 (s), 693 (vs).

$[Pd(Ph_2PCH_2CH_2PPh_2)(S-t-Bu)(C_6H_4-4-OMe)]$ (5**).** The product was obtained in 57.2% (54.1 mg) yield after crystallization from ether at $-35^\circ C$. 1H NMR (C_6D_6) δ 1.65 (s, 9H), 1.70–1.93 (m, 4H), 3.33 (s, 3H), 6.70 (d, 1.5 Hz, 2H), 6.86–6.99 (m, 8H), 7.02–7.15 (m, 4H), 7.26 (m, 4H), 7.54 (t, 7.9 Hz, 2H), 8.10 (m, 4H); $^{31}P\{^1H\}$ NMR (C_6D_6) δ 43.2 (d, 24 Hz), 33.1 (d, 24 Hz).

$[Pd(Ph_2PCH_2CH_2PPh_2)(S-t-Bu)(C_6H_4-3-OMe)]$ (6**).** The product was obtained in 47.4% (66.7 mg) yield after crystallization from ether at $-35^\circ C$. 1H NMR (C_6D_6) δ 1.66 (s, 9H), 1.62–1.98 (m, 4H), 3.30 (s, 3H), 6.57 (d, 7.8 Hz, 1H), 6.86–7.15 (m, 12H), 7.23 (m, 6H), 7.37 (t, 6.5 Hz, 1H), 8.09 (t, 8.5 Hz, 4H); $^{31}P\{^1H\}$ NMR (C_6D_6) δ 42.8 (d, 19 Hz), 32.5 (d, 19 Hz).

$[Pd(Ph_2PCH_2CH_2PPh_2)(S-t-Bu)(C_6H_4-4-NH_2)]$ (7**).** The product was obtained in 46.1% (58.6 mg) after crystallization by layering a methylene chloride solution with ether at $-35^\circ C$. 1H NMR (C_6D_6) δ 1.67 (s, 9H), 1.62–1.92 (m, 4H), 2.57 (s, 2H), 6.28 (dd, 6.2, 2.2 Hz, 2H), 6.88–7.20 (m, 12H), 7.29 (m, 4H), 7.39 (t, 7.7 Hz, 2H), 8.14 (dd, 1.3, 2.1 Hz, 4H); $^{31}P\{^1H\}$ NMR (C_6D_6) δ 31.94 (d, 24.2 Hz), 41.57 (d, 24.2 Hz); IR (KBr, cm^{-1}) 3454 (m), 3375 (m), 3329 (w), 3047 (m), 3002 (m), 2944 (m), 2904 (m), 2880 (m), 2843 (m), 1611 (m), 1583 (m), 1478 (s), 1432 (s), 1263 (s), 1151 (m), 1098 (s), 697 (vs).

$[Pd(Ph_2PCH_2CH_2PPh_2)(S-t-Bu)(C_6H_4-3-NH_2)]$ (8**).** The product was obtained in 56.9% (61.3 mg) yield after crystallization by layering a methylene chloride solution with ether at $-35^\circ C$. 1H NMR (C_6D_6) δ 1.69 (s, 9H), 1.69–1.95 (m, 4H), 2.61 (s, 2H), 6.10 (d, 7.8 Hz, 1H), 6.80 (td, 7.5, 2.9 Hz, 1H), 6.87–7.31 (m, 18H), 8.11 (m, 4H); $^{31}P\{^1H\}$ NMR (C_6D_6) δ 31.65 (d, 24.2 Hz), 41.86 (d, 24.2 Hz); IR (KBr, cm^{-1}) 3434 (m), 3417 (m), 3357 (w), 3047 (m), 2943 (m), 2944 (m), 2906 (m), 2879 (m), 1608 (m), 1571 (s), 1465 (m), 1434 (s), 1153 (s), 1101 (s), 747 (vs).

$[Pd(Ph_2PCH_2CH_2PPh_2)(S-t-Bu)(C_6H_4-4-CF_3)]$ (9**).** Complex **9** was too reactive to isolate and was therefore generated in situ and spectroscopically analyzed in solution. To a vial was added 4.9 mg (0.0067 mmol) of $[Pd(DPPE)(C_6H_4-4-CF_3)(Br)]$ and 1.0 mg (0.0089 mmol) of 2-methyl-2-propanethiol, sodium salt. C_6D_6 (0.5 mL) was added to this solid mixture and the heterogeneous solution was transferred by pipet into an NMR tube. A clear yellow solution was formed after 0.5 h, and the 1H and $^{31}P\{^1H\}$ NMR spectra showed formation of the product and concomitant formation of $[Pd(DPPE)_2]$ and alkyl sulfide. The yellow solution turned black in solution over the course of several hours at room temperature. 1H NMR (C_6D_6) δ 1.50 (s, 9H), 1.60–1.93 (m, 4H), 6.83–6.97 (m, 10H), 7.03–7.18

(m, 8H), 7.70 (t, 7.8 Hz, 2H), 8.10 (td, 7.1, 1.4, 4H); $^{31}\text{P}\{^1\text{H}\}$ NMR (C_6D_6) δ 33.89 (d, 24.2 Hz), 44.19 (d, 24.2 Hz).

[Pd(Ph₂PCH₂CH₂PPh₂)(S-*t*-Bu)(2,4-(CH₃)₂C₆H₃)] (10). The product was obtained in 55.2% (48.6 mg) yield after crystallization by layering a toluene solution with pentane at -35°C . ^1H NMR (C_6D_6) δ 1.44 (m, 2H), 1.65 (s, 9H), 1.91 (m, 2H), 2.17 (s, 3H), 2.44 (s, 3H), 6.56 (d, 8 Hz, 1H), 6.57 (virtual t, 9 Hz, 2H), 6.71 (s, 1H), 6.78 (td, $J_t = 8$ Hz, $J_d = 2.1$ Hz, 2H), 6.89–7.13 (m, 1H), 7.70–7.73 (m, 3H), 8.06 (virtual t, 9 Hz, 2H), 8.22 (virtual t, 9 Hz, 2H); $^{31}\text{P}\{^1\text{H}\}$ NMR (C_6D_6) δ 40.3 (d, 26 Hz), 31.3 (d, 26 Hz).

[Pd(Ph₂PCH₂CH₂PPh₂)(S-*t*-Bu)(3,4-(CH₃)₂C₆H₃)] (11). The product was obtained in 55.2% (84.5 mg) yield after crystallization by layering a toluene solution with pentane at -35°C . ^1H NMR (C_6D_6) δ 1.66 (s, 9H), 1.70–1.94 (m, 4H), 1.94 (s, 3H), 2.06 (s, 3H), 6.79 (dd, 2.2 Hz, 7.5 Hz, 1H), 6.85–7.28 (m, 17H), 7.54 (t, 7.6 Hz, 1H), 8.12 (dd, 13.3 Hz, 8 Hz, 4H); $^{31}\text{P}\{^1\text{H}\}$ NMR (C_6D_6) δ 42.5 (d, 24 Hz), 31.7 (d, 24 Hz).

[Pd(Ph₂PCH₂CH₂PPh₂)(S-*t*-Bu)(2,6-(CH₃)₂C₆H₃)] (12). The product was obtained in 70.4% (92.3 mg) yield after crystallization by layering a toluene solution with pentane at -35°C . ^1H NMR (C_6D_6) δ 1.58 (s, 9H), 1.62–1.84 (m, 4H), 2.65 (s, 6H), 6.78–6.92 (m, 6H), 6.95 (m, 4H), 7.05–7.12 (m, 9H), 8.23 (dd, 9.9 Hz, 8 Hz, 4H); $^{31}\text{P}\{^1\text{H}\}$ NMR (C_6D_6) δ 39.2 (d, 27 Hz), 27.4 (d, 27 Hz).

[Pd(Ph₂PCH₂CH₂PPh₂)(SMe)(C₆H₄-4-Cl)] (13). The product was obtained in 61.7% (86.7 mg) yield after crystallization by layering a toluene solution with pentane at -35°C . ^1H NMR (C_6D_6) δ 1.64–1.95 (m, 4 H), 2.22 (d, 5.6 Hz, 3H), 6.82–7.17 (m, 18H), 7.36 (t, 7.5 Hz, 2H), 8.07 (m, 4H); $^{31}\text{P}\{^1\text{H}\}$ NMR (C_6D_6) δ 36.39 (d, 25.4 Hz), 43.43 (d, 25.4 Hz).

[Pd(Ph₂PCH₂CH₂PPh₂)(S-*t*-Bu)(CH₃)] (14). To a 20 mL vial was added 413.0 mg (0.7441 mmol) of [Pd(DPPE)(Me)(Cl)] and 125.5 mg (1.121 mmol) of 2-methyl-2-propanethiol, sodium salt as solids. This mixture was suspended in 10 mL of THF and stirred at room temperature for 0.5 h. The resulting mixture was filtered through a medium fritted funnel, and the THF was removed under vacuum. The residual solid was dissolved in benzene, and the resulting suspension was filtered through a medium fritted funnel. The product was obtained as crystalline needles by crystallization from benzene layered with pentane at room temperature (392 mg, 86.5%). ^1H NMR (C_6D_6) δ 1.38 (virtual t, 7 Hz, 3H), 1.65–1.98 (m, 4H), 1.90 (s, 9H), 7.20 (m, 12H), 7.47 (dd, 10.0 Hz, 8 Hz, 4H), 7.96 (t, 8 Hz, 4H); $^{31}\text{P}\{^1\text{H}\}$ NMR (C_6D_6) δ 50.3 (d, 21 Hz), 31.5 (d, 21 Hz).

[Pd(Ph₂PCH₂CH₂PPh₂)(S-*t*-Bu)(CHC(CH₃)₂)] (15). Complex 15 was too reactive to isolate in pure form. Pd(PPh₃)₂(CHC(CH₃)₂)(Br) was prepared by stirring a mixture of 570.3 mg (0.7983 mmol) of Pd[(*p*-tolyl)₃]₂^{86,87} and 214.4 mg (1.588 mmol) of 1-bromo-2-methylpropene in 10 mL of benzene followed by addition of 419.2 mg (1.600 mmol) of triphenylphosphine. The solution was filtered through Celite after 1.5 h. [Pd(PPh₃)₂(CHC(CH₃)₂)(Br)] ($^{31}\text{P}\{^1\text{H}\}$ NMR (C_6D_6) δ 25.18 (s)) was isolated by precipitation from pentane followed by filtration through a medium fritted funnel and was used without further purification. Into a 20 mL vial was added 223.1 mg (0.2915 mmol) of Pd(PPh₃)₂(CHC(CH₃)₂)(Br) and 5 mL of benzene. Upon dissolution, 140.4 mg (0.3528 mmol) of DPPE in 2 mL of benzene was added to the solution, and the mixture was stirred for 5 min. [Pd(DPPE)(CHC(CH₃)₂)(Br)] ($^{31}\text{P}\{^1\text{H}\}$ NMR (C_6D_6) δ 50.9 (d, 25.6 Hz), 28.9 (d, 25.6 Hz)) was isolated as a yellow powder by precipitation from pentane followed by filtration through a medium fritted funnel and was used without further purification. To a 20 mL vial was weighed 63.6 mg (0.0995 mmol) of [Pd(DPPE)(CHC(CH₃)₂)(Br)] and 13.4 mg (0.120 mmol) of 2-methyl-2-propanethiol, sodium salt. This mixture was dissolved in 5 mL of THF and stirred at room temperature for 0.5 h. The resulting orange mixture was filtered through Celite, and the THF was removed under vacuum. Crystallization at -35°C from toluene layered with pentane resulted in the formation of an orange solid. ^1H and $^{31}\text{P}\{^1\text{H}\}$ NMR spectra of this solid showed formation of the product along with <5% of Pd(DPPE)₂ and ~10% of the alkyl sulfide. ^1H

NMR (C_6D_6) δ 1.54 (s, 3H), 1.76 (s, 3H), 1.82 (broad s, 4H), 1.97 (s, 9H), 6.5 (dd, $J_{\text{trans}} = 11.4$ Hz, $J_{\text{cis}} = 8$ Hz, 1H), 6.93–7.12 (m, 16H), 8.05 (virtual t, 9.0 Hz, 4H); $^{31}\text{P}\{^1\text{H}\}$ NMR (THF) δ 42.3 (d, 23 Hz), 31.5 (d, 23 Hz).

[Pd(Ph₂PCH₂CH₂PPh₂)(S-*t*-Bu)(CC(CH₂)₃CH₃)] (16). To a 20 mL vial was weighed 192.9 mg (0.2708 mmol) of [Pd(DPPE)(CC(CH₂)₃-CH₃)(I)]. This solid was suspended in 2 mL of THF. A suspension of 2-methyl-2-propanethiol, sodium salt (45.2 mg, 0.136 mmol) in 5 mL of THF was added and the resulting dark orange mixture was stirred for 1 h at room temperature. After this time, the THF solvent was evaporated under vacuum. The residual solid was dissolved in benzene and the mixture was filtered through Celite. The product was obtained as a crystalline orange solid by layering a toluene solution with pentane at -35°C (158 mg, 86.5%). ^1H NMR (C_6D_6) δ 0.79 (t, 7 Hz, 3H), 1.28–1.42 (m, 4H), 1.69–1.89 (m, 4H), 2.22 (s, 9H), 2.34 (t, 6 Hz, 2H), 7.00–7.03 (m, 12H), 7.84–7.92 (m, 8H); $^{31}\text{P}\{^1\text{H}\}$ NMR (C_6D_6) δ 47.1 (d, 22 Hz), 44.3 (d, 22 Hz); IR (KBr, cm^{-1}) 2120 (w).

[Pd(Ph₂PCH₂CH₂PPh₂)(S-*t*-Bu)(CCC₆H₅)] (17). The product was obtained in 48.2% (48.8 mg) yield after crystallization by layering a toluene solution with pentane at -35°C . ^1H NMR (C_6D_6) δ 1.77–1.82 (m, 4H), 2.21 (s, 9 H), 6.92–7.35 (m, 15H), 7.33 (d, 7.3 Hz, 2H), 7.85 (m, 8H); $^{31}\text{P}\{^1\text{H}\}$ NMR (C_6D_6) δ 48.1 (d, 22 Hz), 45.1 (d, 22 Hz); IR (KBr, cm^{-1}) 2100 (w).

[Pd(Ph₂PCH₂CH₂PPh₂)(SCH₃)(CH₃)] (18). The product was obtained in 53.3% (53.6 mg) yield after crystallization by layering a THF solution with ether at -35°C . ^1H NMR (C_7D_8) δ 0.97 (dd, 6 Hz, 7 Hz, 3H), 1.74–1.95 (m, 4H), 2.58 (d, 6 Hz, 3H), 7.30–7.36 (m, 12H), 7.49 (virtual t, 9.8 Hz, 4H), 8.00 (virtual t, 10 Hz, 4H); $^{31}\text{P}\{^1\text{H}\}$ NMR (C_7D_8) δ 50.4 (d, 23 Hz), 35.8 (d, 23 Hz).

[Pd(Ph₂PCH₂CH₂PPh₂)(SC₆H₄-4-Cl)(C₆H₄-4-*n*-Bu)] (19). **Synthesis of *syn*- and *anti*-[Pd(PPh₃)(C₆H₄-4-*n*-Bu)(μ -OH)]₂.** To a 50 mL culture tube was added 238.5 mg (0.2680 mmol) of *trans*-[Pd(PPh₃)₂(C₆H₄-*n*-Bu)(I)] and 156.6 mg (0.9321 mmol) of CsOH·H₂O. This mixture was stirred for 18 h in 35 mL of THF at room temperature after which time the solution was filtered through Celite. The THF was then evaporated under vacuum, and the resultant pale yellow solid was dissolved in 2 mL of benzene. This benzene solution was poured in a vial containing 15 mL of pentane and the mixture stirred for 1 h at room temperature. After this time, a white solid precipitated out of solution. The product was obtained by layering a toluene solution with pentane at -35°C in 69.8% (96.9 mg) yield ($^{31}\text{P}\{^1\text{H}\}$ NMR (C_6D_6) δ 34.66 (s), 33.78 (s), relative intensity = 2:1).

To a 20 mL vial was added 80.2 mg (0.0776 mmol) of *syn*- and *anti*-[Pd(PPh₃)(C₆H₄-4-*n*-Bu)(μ -OH)]₂ and 5 mL of THF. A solution of 4-chlorothiophenol (26.1 mg, 0.181 mmol) in 5 mL of THF was added to the *n*-butyl aryl hydroxy dimer solution and stirred for 5 min. The resultant brown solution was identified as *syn*- and *anti*-[Pd(PPh₃)(C₆H₄-4-*n*-Bu)(μ -SC₆H₄-4-Cl)]₂ ($^{31}\text{P}\{^1\text{H}\}$ (THF) δ 28.4 (s), 27.3 (s), relative intensity = 1:1.5). To this solution was added 68.6 mg (0.172 mmol) of DPPE and the mixture was stirred for another 5 min, after which time an orange solution was obtained. The THF was removed from this orange solution under vacuum and the resultant orange solid was dissolved in toluene and filtered through Celite. A fluffy pink solid was obtained by layering a toluene solution with pentane at -35°C in 50.0% (60.4 mg) yield. ^1H NMR (C_6D_6) δ 0.93 (t, 7.3 Hz, 3H), 1.27 (m, 2H), 1.49 (m, 2H), 1.80 (m, 4H), 2.37 (t, 7.6 Hz, 2H), 6.56 (dd, 7.7 Hz, 1.8 Hz, 2H), 6.71 (d, 8.4 Hz, 2H), 6.92 (m, 7H), 7.13 (m, 11H), 7.41 (d, 8.4 Hz, 2H), 7.93 (m, 4H); $^{31}\text{P}\{^1\text{H}\}$ NMR (C_6D_6) δ 45.06 (d, 24.4 Hz), 35.31 (d, 24.4 Hz).

[Pd(Ph₂PCH₂CH₂PPh₂)(SC₆H₅)(C₆H₄-4-*n*-Bu)] (20). The product was obtained in 86.0% (105.8 mg) yield by layering a toluene solution with pentane at -35°C . ^1H NMR (C_6D_6) δ 0.87 (t, 6.9 Hz, 3H), 1.29 (m, 2H), 1.44 (m, 2H), 1.69–1.95 (m, 4H), 2.36 (t, 7.4 Hz, 2H), 6.59 (d, 7.1 Hz, 2H), 6.78–6.99 (m, 10H), 7.02–7.12 (m 5H), 7.20–7.30 (m, 6H), 6.67 (d, 7.4 Hz, 2H), 7.99 (t, 7.9 Hz, 4H); $^{31}\text{P}\{^1\text{H}\}$ NMR (C_6D_6) δ 44.51 (d, 24.4 Hz), 34.59 (d, 24.4 Hz).

[Pd(Ph₂PCH₂CH₂PPh₂)(SC₆H₄-4-CH₃)(C₆H₄-4-*n*-Bu)] (21). The product was obtained in 70.5% (81.4 mg) yield after crystallization by layering a toluene solution with pentane at -35°C . ^1H NMR (C_6D_6) δ 0.88 (t, 7.2 Hz, 3H), 1.25 (m, 2H), 1.45 (m, 2H), 1.82 (m, 4H), 2.06 (s, 3H), 2.37 (t, 7.8 Hz, 2H), 6.60 (m, 4H), 6.85–6.99 (m, 6H), 7.02–

(87) Paul, F.; Patt, J.; Hartwig, J. F. *J. Am. Chem. Soc.* **1994**, *116*, 5659–5670.

(88) Paul, F.; Patt, J.; Hartwig, J. F. *Organometallics* **1995**, *14*, 3030–3039.

7.13 (m, 6H), 7.21–7.31 (m, 6H), 7.56 (d, 7.9 Hz, 2H), 8.00 (m, 4H); $^{31}\text{P}\{\text{H}\}$ NMR (C_6D_6) δ 44.08 (d, 24 Hz), 34.57 (d, 24 Hz).

[Pd(Ph₂PCH₂CH₂PPh₂)(SC₆H₄-4-OCH₃)(C₆H₄-4-*n*-Bu)] (22). The product was obtained in 70.9% (75.5 mg) yield after crystallization by layering a toluene solution with pentane at –35 °C. ^1H NMR (C_6D_6) δ 0.89 9 (t, 7.2 Hz, 3H), 1.27 (m, 2H), 1.46 (m, 2H), 1.71–1.95 (m, 4H), 2.37 (t, 7.5 Hz, 2H), 3.27 (s, 3H), 6.40 (d, 8.5 Hz, 2H), 6.61 (d, 7.4 Hz, 2H), 6.87–7.0 (m, 7H), 7.02–7.31 (m, 11H), 7.52 (d, 8.4 Hz, 2H), 8.01 (t, 8.6 Hz, 4H); $^{31}\text{P}\{\text{H}\}$ NMR (C_6D_6) δ 43.79 (d, 24 Hz), 34.68 (d, 24 Hz).

[Pd(Ph₂PCH₂CH₂PPh₂)(Ph)(S-(C₆H₃-2,4-(CH₃)₂))] (23). The product was obtained in 51.8% (62.7 mg) yield after crystallization by layering a 10:1 toluene:THF mixture with pentane at –35 °C. ^1H NMR (C_6D_6) δ 1.69–1.93 (m, 4H), 2.09 (s, 3H), 2.69 (s, 3H), 6.70 (d, 1.2 Hz, 1H), 6.72 (m, 3H), 6.83–6.93 (m, 6H), 7.06–7.12 (m, 5H), 7.17–7.27 (m, 5H), 7.29–7.34 (m, 3H), 7.69 (d, 7.8 Hz, 1H), 7.99 (td, 10.1, 1.4 Hz, 4H); $^{31}\text{P}\{\text{H}\}$ NMR (C_6D_6) δ 43.9 (d, 24 Hz), 34.7 (d, 24 Hz).

[Pd(Ph₂PCH₂CH₂PPh₂)(Ph)(S-(C₆H₃-3,4-(CH₃)₂))] (24). The product was obtained in 47.6% (53.7 mg) yield after crystallization by layering a 10:1 toluene:THF mixture with pentane at –35 °C. ^1H NMR (C_6D_6) δ 1.79–1.94 (m, 4H), 1.87 (s, 3H), 1.95 (s, 3H), 6.62 (d, 7.7 Hz, 1H), 6.70–6.79 (m, 3H), 6.84–6.93 (m, 6H), 7.04–7.11 (m, 5H), 7.19–7.27 (m, 5H), 7.33 (s, 1H), 7.40 (t, 7 Hz, 2H), 7.49 (d, 7.4 Hz, 1H), 7.98 (virtual t, 9 Hz, 4H); $^{31}\text{P}\{\text{H}\}$ NMR (C_6D_6) δ 44.3 (d, 25 Hz), 35.3 (d, 25 Hz).

[Pd(Ph₂PCH₂CH₂PPh₂)(Ph)(S-(C₆H₃-2,6-(CH₃)₂))] (25). The product was obtained in 35.3% (58.6 mg) yield after crystallization by layering a toluene solution with pentane at –35 °C. ^1H NMR (C_6D_6) δ 1.72–1.95 (m, 4H), 2.81 (s, 6H), 6.64–6.66 (m, 3H), 6.82–6.92 (m, 2.0 Hz, 6H), 6.94 (t, 7.4 Hz, 3H), 6.82–6.97 (m, 9H), 8.05–8.11 (m, 4H); $^{31}\text{P}\{\text{H}\}$ NMR (C_6D_6) δ 44.7 (d, 25 Hz), 35.8 (d, 25 Hz).

[Pd(Ph₂P(C₆H₄)PPh₂)(S-*t*-Bu)(C₆H₄-4-Me)] (26). The product was obtained in 85.1% (98.9 mg) yield after crystallization by layering a toluene solution with pentane at –35 °C. ^1H NMR (C_6D_6) δ 1.58 (s, 9H), 2.15 (s, 3H), 6.77–6.94 (m, 10H), 7.02–7.10 (m, 6H), 7.26–7.32 (m, 5H), 7.41 (m, 1H), 7.57 (t, 7.8 Hz, 2H), 7.96 (m, 4H); $^{31}\text{P}\{\text{H}\}$ NMR (C_6D_6) δ 43.60 (d, 24.2 Hz), 46.43 (d, 24.2 Hz).

[Pd(Ph₂PCH₂CH₂CH₂PPh₂)(S-*t*-Bu)(CH₃)] (27). The product was obtained in 34.8% (37.8 mg) yield after crystallization from a toluene solution layered with pentane at –35 °C. ^1H NMR (C_6D_6) δ 1.20 (virtual t, 7.6 Hz, 3H), 1.24–1.35 (m, 2H), 1.71 (s, 9H), 1.87–1.93 (m, 4H), 7.00–7.15 (m, 12 H), 7.53 (m, 4H), 7.84 (virtual t, 8 Hz, 4H); $^{31}\text{P}\{\text{H}\}$ NMR (C_6D_6) δ 15.8 (d, 50 Hz), –4.9 (d, 50 Hz).

[Pd(Ph₂P(C₆H₄)PPh₂)(S-*t*-Bu)(CH₃)] (28). The product was obtained in 36.8% (80.1 mg) yield after crystallization by layering a THF solution with ether at –35 °C. ^1H NMR (C_6D_6) δ 1.50 (virtual t, 7.2 Hz, 3H), 1.86 (s, 9H), 6.79 (broad s, 2H), 6.89–7.08 (m, 12H), 7.19–7.38 (m, 2H), 7.54 (dd, 9.6 Hz, 8 Hz, 4H), 7.85 (virtual t, 8 Hz, 4H); $^{31}\text{P}\{\text{H}\}$ NMR (C_6D_6) δ 51.6 (d, 22 Hz), 40.7 (d, 22 Hz).

[Pd(Ph₂P((C₅H₄)₂Fe)PPh₂)(S-*t*-Bu)(CH₃)] (29). The product was obtained in 13.7% (23.5 mg) yield after crystallization by layering a THF solution with ether at –35 °C. The orange powder turned brown overnight in the drybox at room temperature precluding elemental analysis. ^1H NMR (C_6D_6) δ 1.31 (virtual t, 7.6 Hz, 3H), 1.97 (s, 9H), 3.72–3.73 (t, 1.7 Hz, 2H), 3.85–3.88 (m, 4H), 4.32 (t, 2.0 Hz, 2H), 7.02–7.18 (m, 12H), 7.71–7.78 (m, 4H), 8.12–8.15 (virtual t, 9.6 Hz, 4H); $^{31}\text{P}\{\text{H}\}$ NMR (C_6D_6) δ 27.9 (d, 34 Hz), 7.6 (d, 34 Hz).

[Pd(Ph₂PCH₂(C₁₈H₁₀)CH₂PPh₂)(S-*t*-Bu)(CH₃)] (30). To a Schlenk tube was added 50.9 mg (0.0539 mmol) of [Pd(PPh₃)(Me)(μ -S-*t*-Bu)]⁵² and 70.1 mg (0.112 mmol) of TRANSPOS in 5 mL of benzene. The reaction mixture was stirred for 7 h at 85 °C after which time it was filtered through Celite. The product (78.6 mg, 87.5%) was isolated as a yellow powder by layering a benzene solution with pentane at room temperature. ^1H NMR (C_6D_6) δ (virtual t, 5.8 Hz, 3H), 1.20 (s, 9H), 3.50 (dt, $J_d = 12.3$ Hz, $J_t = 4$ Hz, 2H), 6.15 (m, 2H), 6.64 (d, 8.0 Hz, 2H), 6.73 (t, 7 Hz, 4H), 6.83 (d, 7.2 Hz, 2H), 7.15–7.26 (m, 6H), 7.22–7.27 (m, 4H), 7.54 (d, 8.2 Hz, 2H), 7.58 (d, 8.6 Hz, 2H), 7.64 (d, 8.4 Hz, 2H), 7.90–7.96 (m, 4H), 10.4 (broad s, 2H); $^{31}\text{P}\{\text{H}\}$ NMR (C_6D_6) δ 23.3 (s).

Phosphine Dependence on the Reductive Elimination of 1. Into four small vials were weighed 2.4 mg (0.0036 mmol) of **1**. Four

samples of PPh₃-*d*₁₅ were weighed into four different vials: 5 mg (0.02 mmol), 10 mg (0.04 mmol), 20 mg (0.07 mmol), and 40 mg (0.1 mmol). A sample of the thiolate complex and a sample of PPh₃-*d*₁₅ were dissolved in 0.6 mL of C₆D₆. Upon dissolution, the solution was transferred to a screw capped NMR tube. Reaction rates were measured by ^1H NMR spectroscopy at 50 °C. Samples were shimmed at room temperature and removed from the probe. The NMR probe was then heated to 50 °C. The sample was placed into the probe and quickly reshimmied, and an automated program was initiated that collected single pulse experiments at different time intervals. The concentration of **1** was measured by integration of the *tert*-butyl resonance relative to the trimethoxybenzene internal standard. The following rate constants were obtained for [**1**] = 0.0060 M at different concentrations of PPh₃-*d*₁₅: ($k(\pm 0.2)$, [PPh₃-*d*₁₅]): $2.5 \times 10^{-4} \text{ s}^{-1}$, 0.060 M; $2.1 \times 10^{-4} \text{ s}^{-1}$, 0.12 M; $2.2 \times 10^{-4} \text{ s}^{-1}$, 0.24 M.

Phosphine Dependence on the Reductive Elimination of 14. A stock solution was prepared by dissolving 31.5 mg (0.0518 mmol) of **14** in approximately 2 mL of C₆D₆, transferring the solution to a 3 mL volumetric flask, and adding C₆D₆ to make a 3.0 mL solution with [**14**] = 0.017 M. Four samples of PPh₃-*d*₁₅ were weighed separately into four different vials. A 0.5 mL aliquot of the volumetric solution was transferred by syringe to the vial containing the phosphine. Upon dissolution of the phosphine, the solution was transferred to an amber NMR tube. The tube was frozen in liquid N₂ and flame sealed. These sealed tubes were immersed in a constant temperature water bath at 95 °C. The concentration of **14** was measured by integration of the *tert*-butyl resonance relative to the trimethoxybenzene internal standard by ^1H NMR spectroscopy. The following rate constants were obtained at different concentrations of PPh₃-*d*₁₅ (k , [PPh₃-*d*₁₅]): $(2.1 \pm 0.2) \times 10^{-5} \text{ s}^{-1}$, 0.082 M; $(1.82 \pm 0.04) \times 10^{-5} \text{ s}^{-1}$, 0.16 M; $(2.02 \pm 0.03) \times 10^{-5} \text{ s}^{-1}$, 0.25 M; $(1.91 \pm 0.06) \times 10^{-5} \text{ s}^{-1}$, 0.33 M.

Kinetic Analysis of the Reductive Elimination Reaction of 1–9. The palladium thiolate complexes and PPh₃-*d*₁₅ were weighed into a vial: 2.4 to 3.6 mg of **1–8** and 10 equiv of PPh₃-*d*₁₅ were dissolved in 0.6 mL of C₆D₆. The solution was transferred into a screw capped NMR tube. To a screw-capped NMR tube was added a freshly prepared sample of **9** and 10 equiv of PPh₃-*d*₁₅. Reaction rates were measured by ^1H NMR spectroscopy at 50 °C as described above. The results of the kinetic analysis are summarized in Table 5.

Kinetic Analysis of the Reductive Elimination Reaction of 19–22. The palladium thiolate complexes and PPh₃-*d*₁₅ were weighed into a vial: 5.2 mg (0.0067 mmol) of **19** and 3.9 mg (0.014 mmol) of PPh₃-*d*₁₅; 4.5 mg (0.0050 mmol) of **20** and 3.6 mg (0.13 mmol) of PPh₃-*d*₁₅; 4.2 mg (0.0055 mmol) of **21** and 4.0 mg (0.14 mmol) of PPh₃-*d*₁₅; 3.4 mg (0.0044 mmol) of **22** and 3.2 mg (0.012 mmol) of PPh₃-*d*₁₅. Upon dissolution in 0.5 mL of C₆D₆, the mixture was transferred into a screw capped NMR tube. Reaction rates were measured by ^1H NMR spectroscopy at 70 °C as described above. The results of the kinetic analysis are summarized in Table 6.

Kinetic Analysis of the Reductive Elimination of 1 with Trapping Reagents. Into a vial was weighed 5.0 mg (0.0075 mmol) of **1** and 10 equiv of *p*-iodotoluene. This mixture was dissolved in 0.6 mL of C₆D₆ and transferred into a screw capped NMR tube. The rate of the reaction was measured by ^1H NMR spectroscopy at 50 °C as described above. The observed rate constant was $1.0 \times 10^{-4} \text{ s}^{-1}$. Similarly, the rate constant for the thermolysis of 5.0 mg (0.0075 mmol) of **1** and 10 equiv of phenylacetylene in 0.6 mL of C₆D₆ at 50 °C was $1.7 \times 10^{-4} \text{ s}^{-1}$.

Thermolysis of 2 at Various Temperatures. Complex **2** and PPh₃-*d*₁₅ were weighed into a vial: 2.6 to 6.4 mg of **2** and 12.6–13.4 mg of PPh₃-*d*₁₅ were dissolved in 0.6 mL of C₆D₆. The solution was transferred into a screw capped NMR tube. Reaction rates were measured by ^1H NMR spectroscopy as described above. The following are rate constants for the thermolysis of **2** were obtained at different temperatures (k , [**2**], [PPh₃-*d*₁₅], $T(\pm 0.5 \text{ K})$): $3.7 \times 10^{-5} \text{ s}^{-1}$, 0.0093 M, 0.045 M, 313 K; $1.3 \times 10^{-4} \text{ s}^{-1}$, 0.0080 M, 0.048 M, 323 K; $4.5 \times 10^{-3} \text{ s}^{-1}$, 0.0096 M, 0.047 M, 333 K; $1.4 \times 10^{-3} \text{ s}^{-1}$, 0.020 M, 0.047 M, 343 K.

Thermolysis of 10–12, 15–17, 23–25, and 27–30. Samples were performed in screw capped NMR tubes immersed in oil baths of constant temperature or in sealed NMR tubes completely submerged

in a constant water bath. Reactions were monitored at many timed intervals by the ^1H NMR spectroscopy. Concentrations of the starting materials were determined by integrating the *tert*-butyl or methyl resonances of the starting materials with respect to an internal standard, trimethoxybenzene. Half-lives were estimated from the time of reaction to consume half of the starting complex. The palladium thiolato complexes and PPh_3 or $\text{PPh}_3\text{-}d_{15}$ were weighed into a vial: 5.3 mg (0.0076 mmol) of **10** and 3.9 mg (0.015 mmol) of PPh_3 ; 4.9 mg (0.0070 mmol) of **11** and 3.9 mg (0.015 mmol) of PPh_3 ; 4.7 mg (0.0067 mmol) of **12** and 4.0 mg (0.014 mmol) of PPh_3 ; 1.9 mg (0.0026 mmol) of **23** and 1.9 mg (0.0069 mmol) of $\text{PPh}_3\text{-}d_{15}$; 1.9 mg (0.0026 mmol) of **24** and 1.9 mg (0.0069 mmol) of $\text{PPh}_3\text{-}d_{15}$; 2.0 mg (0.0029 mmol) of **25** and 2.2 mg (0.0079 mmol) of $\text{PPh}_3\text{-}d_{15}$. Upon dissolution in 0.5 mL of C_6D_6 , the mixture was transferred into a screw capped NMR tube and immersed into a 50 °C oil bath. The palladium thiolato complexes and PPh_3 were weighed into a vial: 5.0 mg (0.0078 mmol) of **15** and 3.1 mg (0.012 mmol) of PPh_3 ; 5.0 mg (0.0074 mmol) of **16** and 4.1 mg (0.016 mmol) of PPh_3 ; 5.4 mg (0.0078 mmol) of **17** and 4.5 mg (0.017 mmol) of PPh_3 ; 5.0 mg (0.0068 mmol) of **27** and 3.9 mg (0.015 mmol) of PPh_3 ; 5.0 mg (0.0076 mmol) of **28** and 4.4 mg (0.017 mmol) of PPh_3 ; 2.4 mg (0.0031 mmol) of **29** and 3.2 mg (0.012 mmol) of PPh_3 ; 2.9 mg (0.0035 mmol) of **30** and 3.2 mg (0.012 mmol) of PPh_3 . Upon dissolution in 0.5 mL of C_6D_6 , the mixture was transferred into a 5 mm thin-walled NMR tube. The tube was frozen in liquid N_2 and flame sealed. These sealed tubes were submerged in a constant temperature water bath at 95 °C.

X-ray Structural Determination of 8 and 24. Single crystals of **8** and **24** were mounted on glass fibers and immediately placed in a cold nitrogen stream on the X-ray diffractometer. The X-ray intensity data for **8** were collected on a Rigaku AFC5S diffractometer with graphite monochromated $\text{Mo K}\alpha$ radiation at -60 °C and those for **24** were collected on a Siemens P4/CCD with $\text{Mo K}\alpha$ radiation at -78 °C. For **8**, 7042 reflections were collected and 6754 were unique ($R_{\text{int}} = 0.094$). For **24**, 8258 reflections were collected and 8258 were independent ($R_{\text{int}} = 0.000$). Both structures were solved by direct

methods, expanded using Fourier techniques, and refined by full-matrix least squares. The empirical absorption corrections for both structures were applied by using the program DIFABS. There is a solvent molecule of toluene present in the unit cell of **8** and a solvent molecule of THF in the unit cell of **24**. Both complexes crystallized in the monoclinic crystal system and the space group assignments for both were $P21/n$. The non-hydrogen atoms were refined anisotropically and all hydrogen atoms were treated as idealized contributions. Further experimental details of the X-ray diffraction studies are provided in Table 1. Positional parameters for all atoms, anisotropic thermal parameters, all bond lengths and angles, and fixed hydrogen positional parameters for both structures are given in the Supporting Information.

Acknowledgment. We gratefully acknowledge support from the Department of Energy, a Camille Dreyfus Teacher/Scholar Award, and a National Science Foundation Young Investigator Award with matching funds provided by a DuPont Young Professor Award, a Union Carbide Innovative Recognition Award, Boehringer Ingelheim, and Rohm and Haas. J.F.H. is a fellow of the Alfred P. Sloan Foundation. Johnson-Matthey Alpha/Aesar generously provided a loan of palladium chloride. We also are indebted to Mark Andrews from DuPont for insightful mechanistic suggestions.

Supporting Information Available: Experimental procedures for **2–8**, **10–13**, **17**, **18**, and **20–29**; tables of positional parameters and $B(\text{eq})$, U values, intramolecular distances, intramolecular bond angles, Cartesian coordinates, and torsion or conformational angles for hydrogen and non-hydrogen atoms for **8** and **24** (44 pages, print/PDF). See any current masthead page for ordering information and Web access instructions.

JA981428P